cmgh
CELLULAR AND MOLECULAR GASTROENTEROLOGY AND HEPATOLOGY

ORIGINAL RESEARCH

Inhibitors of Arg-Gly-Asp-Binding Integrins Reduce Development of Pancreatic Fibrosis in Mice

Barbara Ulmasov,[1] Brent A. Neuschwander-Tetri,[1] Jinping Lai,[2] Vladimir Monastyrskiy,[1] Trisha Bhat,[1] Matthew P. Yates,[3] Jonathan Oliva,[3] Michael J. Prinsen,[3] Peter G. Ruminski,[3] and David W. Griggs[3]

[1]Division of Gastroenterology and Hepatology, Department of Internal Medicine, [2]Department of Pathology, [3]Center for World Health and Medicine, Saint Louis University, Saint Louis, Missouri

SUMMARY

Arg-Gly-Asp–binding integrins are critically involved in cerulein-induced pancreatic fibrogenesis in mice, a model of chronic pancreatitis. Small-molecule Arg-Gly-Asp integrin antagonists have the potential to be developed for effective treatment of pancreatic fibrotic diseases.

BACKGROUND & AIMS: Pancreatic stellate cells (PSCs) regulate the development of chronic pancreatitis (CP) and are activated by the cytokine transforming growth factor β (TGFB). Integrins of the αv family promote TGFB signaling in mice, probably by interacting with the Arg-Gly-Asp (RGD) sequence of the TGFB latency-associated peptide, which frees TGFB to bind its cellular receptors. However, little is known about the role of integrins in the development of CP. We investigated the effects of small-molecule integrin inhibitors in a mouse model of CP.

METHODS: We induced CP in C57BL/6 female mice by repeated cerulein administration. An active RGD peptidomimetic compound (Center for World Health and Medicine [CWHM]-12) was delivered by continuous infusion, starting 3 days before or 5 days after cerulein administration began. Pancreata were collected and parenchymal atrophy, fibrosis, and activation of PSCs were assessed by histologic, gene, and protein expression analyses. We measured CWHM-12 effects on activation of TGFB in co-culture assays in which rat PSC cells (large T immortalized cells [LTC-14]) activate expression of a TGFB-sensitive promoter in reporter cells.

RESULTS: Pancreatic tissues of mice expressed messenger RNAs encoding subunits of RGD-binding integrins. Cerulein administration increased expression of these integrins, altered pancreatic cell morphology, and induced fibrosis. The integrin inhibitor CWHM-12 decreased acinar cell atrophy and loss, and substantially reduced fibrosis, activation of PSCs, and expression of genes regulated by TGFB. CWHM-12 also reduced established fibrosis in mice and blocked activation of TGFB in cultured cells.

CONCLUSIONS: Based on studies of a mouse model of CP and cultured PSCs, integrins that bind RGD sequences activate PSCs and promote the development of pancreatic fibrogenesis in mice. Small-molecule antagonists of this interaction might be developed for treatment of pancreatic fibrotic diseases. *(Cell Mol Gastroenterol Hepatol 2016;2:499–518; http://dx.doi.org/10.1016/j.jcmgh.2016.03.004)*

Keywords: Signal Transduction; Pancreas; Inflammation; Peptidomimetic.

Chronic pancreatitis (CP) is a slowly progressive disease that causes substantial loss of quality of life from chronic pain, malnutrition, and diarrhea stemming from exocrine insufficiency and finally endocrine insufficiency over decades. The prevalence of CP is approximately 1/2000 persons, and patients with CP have a shortened survival compared with the general population. Extensive pancreatic fibrosis is the primary pathologic feature of CP.[1] No disease-specific treatments are available, but a major advance in the field was the discovery of specialized cells in the pancreas, named *pancreatic stellate cells* (PSCs), which are responsible for the development of fibrosis upon activation.[2–4]

The published literature strongly supports the central importance of cytokine transforming growth factor β (TGFB) in the activation of PSC and in driving pancreatic fibrogenesis.[5] Triggering of the TGFB pathway is the primary regulatory mechanism found in several fibroproliferative diseases including pulmonary fibrosis and cirrhosis.[6] TGFB initially is produced by cells in an inactive state through association with latency-associated peptide (LAP) and requires activation to produce its effects.[7] The latent complex is abundantly present in most tissues, including the pancreas,[8] and thus activation control may be a more important mechanism of regulating its biological effects than control of expression. Integrins of the αv family bind

Abbreviations used in this paper: **Col1a1, collagen type I α1; CP, chronic pancreatitis; CTGF, connective tissue growth factor; CWHM, Center for World Health and Medicine; DMEM, Dulbecco's modified Eagle medium; DMSO, dimethyl sulfoxide; ECM, extracellular matrix; FBS, fetal bovine serum; IC_{50}, median inhibitory concentration; LAP, latency-associated peptide; LTC-14, large T immortalized cells; MLEC, mink lung epithelial cell; MMP, matrix metallopeptidase; mPSC, mouse pancreatic stellate cell; mRNA, messenger RNA; PBS, phosphate-buffered saline; PCR, polymerase chain reaction; PSC, pancreatic stellate cell; p-SMAD, phosphorylated SMAD; RGD, arginine-glycine-aspartic acid; α-SMA, α-smooth muscle actin; TGFB, transforming growth factor β.**

Most current article

2352-345X
http://dx.doi.org/10.1016/j.jcmgh.2016.03.004

LAP via its Arg-Gly-Asp (RGD) sequence, and have been implicated in TGFB activation in several organs.[9–11] However, the mechanism of TGFB activation in pancreatic fibrogenesis has not been studied.

Integrins are a large family of transmembrane cell adhesion and signaling receptors consisting of α and β subunits connecting the inner cytoskeleton with the outer extracellular matrix.[12] In mammals, a total of 18 α and 8 β integrin subunits noncovalently associate to form 24 different integrin heterodimers. This diversity and complexity allows highly tissue-specific expression of different heterodimers with different ligand affinities. Of the 24 integrin heterodimers, 6 have been shown to bind and activate latent TGFB in vitro by binding to the amino acid sequence RGD of LAP.[13–18] These include all αv integrins (αvβ1, αvβ3, αvβ5, αvβ6, and αvβ8) and α8β1.

The Center for World Health and Medicine (CWHM) at Saint Louis University has synthesized many small-molecule RGD peptidomimetic compounds that inhibit the ligand-binding activities of integrins involved in TGFB activation. One of these compounds, a broad range antagonist of RGD-binding integrins called CWHM-12, recently was tested in mouse models of lung and liver fibrosis and showed significant efficacy in fibrosis prevention and reversal.[11]

The present studies evaluate the effects of pharmacologic inhibition of RGD-binding integrins by CWHM-12 in a cerulein-induced injury mouse model of CP. This model reproduces the histopathologic features found in human CP, including fibrosis, inflammation, acinar atrophy, and tubular complex formation.[19–21] Moreover, the TGFB pathway was shown to play a central role in fibrosis development in this model.[22–24] We show a critical role of RGD-binding integrins in CP and the promising potential to arrest or possibly even reverse pancreatic fibrosis using a pharmacologic approach to inhibiting integrin-mediated TGFB activation.

Materials and Methods

Animals

Experiments were performed with C57BL/6 female 7- to 8-week-old mice obtained from the Jackson Laboratory (Bar Harbor, ME). All mice were housed in standard facilities under controlled conditions of temperature, humidity, and a 12-/12-hour light/dark cycle, and were maintained on standard rodent chow with free access to water. Animal care and all procedures were approved by the Institutional Animal Care and Use Committee of Saint Louis University.

Induction of Pancreatic Fibrosis and Tissue Processing

Mice were divided randomly into treatment groups of 10 animals each. Pancreatic fibrogenesis was induced by repetitive intraperitoneal injections of 50 μg/kg cerulein (Sigma, Saint Louis, MO) as described in detail previously.[25–27] Briefly, cerulein treatments (one intraperitoneal injection every hour for 6 hours) were given to mice every other day so that each animal received 3 courses of the injury agent. The control group received comparable injections of sterile 0.9% sodium chloride (saline). Mice then were euthanized by CO_2 asphyxiation and this was performed 3 days after the last injection to allow resolution of acute changes. Blood was collected by cardiac puncture in heparin tubes (Lithium Heparin Separator MiniCollect; Greiner Bio-One, Kremsmünster, Austria). The pancreas from each mouse was removed, weighed, and divided into sections. Sections were either immediately frozen in liquid nitrogen and stored at -80°C for subsequent protein extraction and Western blot analysis, fixed in 10% neutral buffered formalin solution (Sigma) for histologic analysis, or placed in an RNA stabilization solution (RNAlater; Ambion, Austin, TX) and stored overnight at 4°C for RNA isolation and subsequent real-time quantitative polymerase chain reaction (PCR) assays.

Induction of Acute Pancreatic Injury and Tissue Processing

Mice were divided into groups of 4–6 animals each. To determine the effects of acute pancreatic injury, mice were subjected to a single course of cerulein treatment (ie, 6 hourly intraperitoneal injections of 50 μg/kg each). Sex- and age-matched control mice received comparable injections of sterile saline solution. Nine hours after the first injection, the mice were euthanized by CO_2 asphyxiation and blood was collected by cardiac puncture for amylase analysis. Each pancreas was removed, weighed, and placed in 10% neutral buffered formalin solution (Sigma-Aldrich, St. Louis, MO) for histologic analysis.

Administration of Integrin Antagonist Compounds

The small-molecular-weight integrin antagonist, CWHM-12, and its inactive enantiomer control compound, CWHM-96, were synthesized by the Center for the World Health and Medicine (Saint Louis University, St. Louis, MO). Syntheses and structures of these compounds have been described previously.[11] This prior report also showed that CWHM-12 has excellent potency (median inhibitory concentration [IC_{50}] in the low nanomolar range) against 4 αv integrins (αvβ1, αvβ3, αvβ6, and αvβ8) and integrin α5β1 in in vitro ligand-binding assays, and also has good but somewhat lesser potency against αvβ5 (IC50 $<$ 100 nmol/L). In contrast, the R-isomer of CWHM-12, called CWHM-96, which differs from CWHM-12 only in the orientation of its carboxyl group, did not inhibit any of these integrins in in vitro ligand-binding assays.[11] To evaluate prevention of pancreatic fibrogenesis (preventive mode), CWHM-12 was delivered by continuous infusion at 100 mg/kg/day (50% dimethyl sulfoxide [DMSO], 50% phosphate-buffered saline [PBS]) using Alzet mini-osmotic pumps (Durect, Cupertino, CA) implanted subcutaneously in mice 3 days before the first cerulein treatment. Minipumps with vehicle (50% DMSO, 50% PBS) also were implanted in cerulein-treated and control saline-treated groups of mice. To evaluate the effect of therapeutic rather than preventive compound administration, minipumps with CWHM-12, CWHM-96, or vehicle (for the cerulein- and saline-treated groups) were implanted on day 5 (relative to the first day of cerulein treatment). To evaluate effects on acute pancreatic injury,

CWHM-12 was given to mice by intraperitoneal injection (100 μL of 40 mg/mL CWHM-12 in 50% DMSO, 50% PBS, pH 7.0) starting 1 hour before the first cerulein injection, and then twice more at the same dose at intervals of 3 hours. The control group of mice received intraperitoneal injections of vehicle (50% DMSO, 50% PBS) in place of compound.

Real-Time Quantitative PCR

Isolation of total RNA from pancreatic tissue and real-time quantitative PCR was conducted as we described previously.[27] The primer sequences of transcripts evaluated by quantitative PCR are listed in Table 1. PCR primers were synthesized by Life Technologies (Carlsbad, CA) based on the sequences from Primer Bank.[28] Connective tissue growth factor (CTGF) primers were designed using Primer Express software (Applied Biosystems, Foster City, CA). Results were calculated with normalization to ribosomal protein, large, P0 messenger RNA (mRNA). Ribosomal protein, large, P0 (also known as acidic ribosomal phosphoprotein P0) was chosen as the housekeeping control gene because it previously was shown that its mRNA does not change significantly with single or multiple episodes of cerulein-induced pancreatitis.[29–31] The comparative threshold cycle method [32] was used to calculate changes in mRNA abundance.

Determination of CWHM-12 Concentration in Plasma

Plasma samples (50 uL total volume) were diluted with control naive mouse plasma as appropriate to bring samples into the range of the standard curve. The samples were capped and mixed on a multiplate vortexer for 5 minutes and centrifuged for 5 minutes at 3200 rpm. The supernatant was transferred to a 96-well sample plate and capped for liquid chromatography–mass spectrometry and liquid chromatography - tandem mass spectrometry (LC-MS-MS) analysis using a system consisting of a LC-20AD pump (Shimadzu, Kyoto, Japan), an HTC PAL autosampler (Leap Technologies, Carrboro, NC), and a Sciex API-4000 mass spectrometer in ESI mode (AB Sciex, Foster City, CA). An Amour C18 reverse-phase column (2.1 $\times$ 30 mm, 5 μm; Analytical Sales and Services, Pompton Plains, NJ) was used for chromatographic separation. Mobile phases were 0.1% formic acid (aqueous) and 100% acetonitrile (organic) with a flow rate of 0.35 mL/min. The starting phase was 10% acetonitrile for 0.9 minutes, increased to 90% acetonitrile over 0.4 minutes, maintained for an additional 0.2 minutes, returned to 10% acetonitrile over 0.4 minutes, and then held for 1.6 minutes. The multiple reaction monitoring (MRM) transition for CWHM-12 was as follows: mass/charge (m/z), 590.13 $>$ 234.1. Peak areas were integrated using Analyst 1.5.1 (AB Sciex).

Histology Analysis

Formalin-fixed pancreatic tissues were embedded in paraffin, sectioned, and stained with H&E using standard protocols for microscopic evaluation. Slides were graded by an experienced pathologist (J.L.) masked to treatment groups using a semiquantitative histopathology scoring system. For the pancreatic fibrosis experiments, slides were scored as follows: within pancreatic sections the acinar atrophy/loss was graded as follows: 0, absent; 1, 1%–5%; 2, 6%–15%; 3, 16%–35%; 4, 36%–50%; and 5, more than 50%; necrosis was scored as follows: 0, no necrosis; 1, minimal ($<$10%); 2, moderate (10%–50%); and 3, severe ($>$50%); tubular complex formation was scored as follows: 0, absent; 1, 1%–15%; 2, 6%–15%; 3, 16%–35%; 4, 36%–50%; and 5, more than 50%. In addition, the presence of acute inflammatory cells (mainly neutrophils) and chronic inflammatory cells (mononuclear cells) was graded as follows: 0, absent; 1, minimal; 2, mild; 3, moderate; and 4, severe. H&E-stained pancreatic sections from samples

Table 1. Primer Sequences of Mouse Genes Evaluated by Quantitative Reverse-Transcription PCR

Gene	Forward sequence	Reverse sequence
Rplp0	5′-AGATTCGGGATATGCTGTTGGC-3′	5′-TCGGGTCCTAGACCAGTGTTC-3′
Itgav	5’-CGGGTCCCGAGGGAAGTTA-3’	5’-TGGATGAGCATTCACATTTGAGA-3’
Itga5	5’-TGCAGTGGTTCGGAGCAAC-3’	5’-TTTTCTGTGCGCCAGCTATAC-3’
Itga8	5’-CGTCTCTGTTGCGTCTCGG-3’	5’-ATCCAAGTTGAACGCCAGACA-3’
Itgb1	5’-TGGTCAGCAACGCATATCTGG-3’	5’-GATCCACAAACCGCAACCT-3’
Itgb3	5’-GGCGTTGTTGTTGGAGAGTC-3’	5’-CTTCAGGTTACATCGGGGTGA-3’
Itgb5	5’-GAAGTGCCACCTCGTGTGAA-3’	5’-GGACCGTGGATTGCCAAAGT-3’
Itgb6	5’-ACTGTCTTGGTAGGTAACCTTCA-3’	5’-TGGCTTCATAGCAGTTGCCAC-3’
Itgb8	5’-TGCATGTTGTAACGTCAAGTGA-3’	5’-GATGCTGACACATCAACCAGATA-3’
CTGF	5’-CAGAGTGGAGCGCCTGTT-3’	5’- GGATGCACTTTTTGCCCTTCT-3’
α-SMA	5’-GTCCCAGACATCAGGGAGTAA-3’	5’-TCGGATACTTCAGCGTCAGGA-3’
Vim	5’-TCCACACGCACCTACAGTCT-3’	5’-CCGAGGACCGGGTCACATA-3’
Mmp2	5’-ACCTGAACACTTTCTATGGCTG-3’	5’-CTTCCGCATGGTCTCGATG-3’
Col1a1	5’-GCTCCTCTTAGGGGCCACT-3’	5’-CCACGTCTCACCATTGGGG-3’

Rplp0, ribosomal protein, large, P0.

obtained 9 hours after induction of acute pancreatitis were graded on the following 4 criteria: vacuolization, necrosis, inflammation, and edema. Vacuolization was graded as follows: 0, absent; 1, 5%–14%; 2, 15%–35%; 3, 35%–50%; and 4, more than 50%. Necrosis was graded as follows: 0, absent; 1, periductal necrosis less than 5%; 2, focal necrosis 5%–20% (both periductal and parenchymal); and 3, diffuse necrosis 20%–50%. Inflammation was graded as follows: 0, absence of inflammatory infiltrates; 1, inflammatory infiltration in ducts; 2, inflammatory infiltration in the parenchyma less than 50%; and 3, inflammatory infiltration in the parenchyma more than 50%. Edema was graded as follows: 0, absent; 1, focally increased between lobules; 2, diffusely increased between lobules; and 3, acini disrupted and separated. To evaluate pancreatic collagen content, paraffin-embedded pancreatic sections were stained with Sirius red as we have described previously.[26] Pancreatic sections from all mice were pretreated to remove paraffin and stained with 0.1% Sirius red (F3B) solution in saturated picric acid for 1 hour. Slides then were washed in 2 changes of 0.09 N acetic acid, dehydrated with 3 changes of 100% ethanol, cleared in xylene, and finally mounted in Permaslip (Alban Scientific, Inc, St. Louis, MO). The degree of collagen accumulation was assessed by morphometric analysis[33] using ImageJ software (version 1.37; National Institutes of Health, Bethesda, MD) as we have detailed previously.[26] Briefly, 8–12 nonoverlapping images (the number of images needed to cover the whole section) from each pancreatic section were captured using a Leica DM4000 B microscope (Wetzlar, Germany) equipped with a QICAM FAST 1394 (Surrey, British Columbia, Canada) digital camera using the ×20 objective. To measure Sirius red–positive staining, the examination area was chosen and kept constant for all images, the same threshold was applied to all images, and the integrated density for each image was calculated by the program. An image of a blank area of the slide was used for background correction. The amount of collagen was expressed relative to the amount of collagen in the saline-treated control group.

Immunohistochemistry

Formalin-fixed pancreatic tissue sections were pretreated to remove paraffin by standard methods. Endogenous peroxidase activity was blocked by incubation in 3% H_2O_2 at room temperature for 1 hour. Antigen retrieval was performed by a high-temperature unmasking procedure using citrate-based Antigen Unmasking Solution (Vector Laboratories, Inc, Burlingame, CA). Immunologic staining of the sections was conducted using Elite Universal Vectastain ABC kit (Vector Laboratories, Inc) according to the manufacturer's instructions. The antibody to α-smooth muscle actin (α-SMA) was obtained from Sigma (A2547; Sigma). The antibody to the αv subunit was obtained from Bioss (bs-2250R; Woburn, MA). The antibody to vimentin was obtained from Sigma (v-2258). Secondary antibody peroxidase activity was detected with diaminobenzidine solution (BioGenex, Fremont, CA), and slides were counterstained with Hematoxylin Solution, Gill no. 3 (Sigma). Sections were dehydrated and mounted with Permaslip Mounting Medium (Alban Scientific). Images were captured using a Leica DM4000 B microscope equipped with a QICAM FAST 1394 digital camera using the ×20 or ×40 objectives.

Immunofluorescence

For immunofluorescent staining of paraffin-embedded tissues, paraffin removal and antigen retrieval was conducted as described for immunohistochemical staining. Anti–α-SMA and antivimentin antibodies are described in the Immunohistochemistry section. Secondary antibody conjugated with Cy3 for the detection of α-SMA–bound primary antibody was obtained from Jackson Immuno–Research (West Grove, PA) and secondary antibody conjugated with fluorescein isothiocyanate for detection of vimentin-bound primary antibody was obtained from Sigma (F-9259). 4′,6-diamidino-2-phenylindole for nuclear counterstain was obtained from ThermoScientific (Waltham, MA).

Images were captured using a Leica DM4000 B microscope equipped with a QICAM FAST 1394 digital camera using the ×20 objective.

Apoptotic Cell Detection in Pancreatic Tissues

Apoptotic cells in pancreatic tissues were detected by labeling and detecting DNA strand breaks by the terminal deoxynucleotidyl transferase–mediated deoxyuridine triphosphate nick-end labeling method using the ApopTag Peroxidase Detection Kit (Millipore, Temecula, CA) according to the manufacturer's instructions. Stained apoptotic cells with acinar morphology were counted by an experienced pathologist masked to the treatment groups. Ten high-power fields on each tissue section were used for counting.

Western Blot

Western blot was conducted as we described previously[27] using the following primary antibodies: α-SMA, A2547, 1:1000 (Sigma); HDAC1, H3284, 1:1000 (Sigma); phophorylated SMAD3 (p-SMAD3), ab52903, 1:1000 (Abcam, Cambridge, MA). Protein band intensities were quantified using ImageJ software version 1.46 (National Institutes of Health).

Plasma Amylase Activity

Amylase activity in mouse plasma was measured using the Phadebas Amylase Test kit (Pharmacia Diagnostics AB, Uppsala, Sweden) according to the manufacturer's protocol, and expressed as the fold-increase over the amylase activity in the control saline-treated group of mice.

Hematologic Analysis

Cell counts from EDTA-anticoagulated, room-temperature, whole-blood samples were determined for each mouse using an Abbot Cell-Dyn 3700 automated hematology analyzer (GMI, Ramsey, MN).

Zymography

Using a Bead Beater (Biospec Products, Bartlesville, OK), 2-mm zirconia beads, and Eppendorf LoBind low-protein–binding tubes, fresh-frozen pancreases were homogenized for 1 minute at 25 mg/mL in 50 mmol/L Tris-HCl, pH 7.4, 20 mmol/L $CaCl_2$, 0.05% Brij35, and 0.25% Triton X-100 (Sigma-Aldrich, Saint Louis, MO). The homogenate was centrifuged at 18,000×g for 5 minutes at 4°C and then placed on ice. The protein of each homogenate was determined using the Pierce 660-nm Protein Assay Reagent (ThermoFisher Scientific, Waltham, MA). Homogenate samples were mixed with 2× Tris-glycine loading buffer (ThermoFisher Scientific) and normalized to the sample with the lowest protein content using water. Novex-Zymogram precast 10% gels (ThermoFisher Scientific) were loaded with 2 ng of matrix metalloproteinase (MMP)-2 (BioLegend, San Diego, CA) and 9 ug of each of the pancreas homogenates. Gels were run for 100 minutes at 125 V using Tris-glycine sodium dodecyl sulfate running buffer (ThermoFisher Scientific), followed by 3 successive 60-mL washes using 2.5% Triton X-100 in water for 15 minutes. The gel was incubated in 50 mmol/L Tris-HCl pH 7.4 with 10 mmol/L $CaCl_2$ for 40 hours at 37°C to activate the gelatinases, and then stained with 0.1% Coomassie R-250 in 40% ethanol/10% acetic acid for 1 hour at room temperature. The gel was de-stained in 25% ethanol/10% acetic acid for 45 minutes, followed by a second destaining with 5% ethanol/7.5% acetic acid for 4 hours. The gel was imaged on a ChemiDoc XRS+ System (Bio-Rad, Hercules, CA).

Isolation and Culture of Mouse Primary PSCs

Pancreata of ten 7- to 9-week-old C57BL/6J mice were combined for mouse PSC (mPSC) isolation. mPSCs were isolated using collagenase digestion and gradient centrifugation as we described previously.[25] In one set of experiments, isolated quiescent cells were used directly for real-time PCR analysis. In another set of experiments, isolated cells were plated on 100-mm plastic culture plates and were maintained in 10% fetal bovine serum (FBS) in Dulbecco's modified Eagle medium (DMEM; Sigma-Aldrich) with antibiotics (100 U penicillin, 0.1 mg/mL streptomycin) in a humidifying incubator with a 5% CO_2–enriched atmosphere at 37°C. PSCs were cultured for 9 days, plated on 24-well plates (Corning, Corning, NY), and cultured for another 48 hours. Cells were serum-starved for 48 hours and then treated either with 10% FBS media or serum-free media for another 24 hours. RNA was extracted using TRIzol reagent (Life Technologies) and used for real-time quantitative PCR analysis.

Co-culture Bioassay to Measure TGFB Activation

Mink lung epithelial cells (MLECs) stably transfected with a luciferase reporter gene with expression driven by a portion of the plasminogen activator inhibitor promoter were used to assay for the activation of latent TGFB produced in co-culture with a PSC cell line. MLECs were provided by Dr Rifkin (New York University, New York, NY)[34] and co-cultured rat PSC cell line LTC-14 was obtained from Dr Sparmann (University of Rostock, Rostock, Germany).[35] MLECs were seeded at 1.5×10^4 cells/well on a 96-well, flat-bottom, white-walled tissue culture plate (Corning) in 50 μL of DMEM supplemented with 10% FBS, penicillin, and streptomycin, and allowed to attach for 1 hour. LTC-14 cells were seeded on top of the MLECs in equal volume at a density of 5×10^4 cells/well and were incubated for 20 hours in a humidifying incubator with a 5% CO_2–enriched atmosphere at 37°C. After incubation, media was aspirated and cells were lysed in 50 μL of Glo Lysis Buffer (Promega, Madison, WI) for 5 minutes. Next, an equal volume of Bright-Glo-Reagent (Bright-Glo Luciferase Assay System; Promega) was added to the lysis buffer and luciferase activity was measured using a SpectraMax-L plate reader (Molecular Devices, Sunnyvale, CA). Relative luciferase activity was presented as the fold-increase over the average of baseline luciferase activity (MLECs only). As assay controls, TGFB neutralizing antibody (clone 1D11; R&D Systems, Minneapolis, MN) or IgG1 isotype-matched control antibody (clone 11711; R&D Systems) were added at the start of the MLEC–LTC-14 co-culture to a final concentration of 50 μg/mL. CWHM-12 and CWHM-96 control compound were diluted in serum-free DMEM to obtain the desired concentrations and added to MLEC–LTC-14 co-cultures at the start of the experiment. Relative luciferase activity values were imported into GraphPad Prism software (La Jolla, CA) for generation of dose-response curves and calculation of IC_{50} values.

Statistical Analysis

The nonparametric *U* test was used for statistical analysis of histologic measures of chronic and acute pancreatitis. Statistical analysis of data for all other experiments was performed using 1-way analysis of variance followed by a 2-tailed *t*-test (software version 3.1; SigmaStat, San Jose, CA). For quantitative PCR results, ΔC_T values were used for statistical analysis, as recommended.[36] Data are expressed as means ± SEM.

All authors had access to the study data and reviewed and approved the final manuscript.

Results

Expression of RGD-Binding Integrin Subunits in Mouse Pancreas in the Cerulein Model of Pancreatic Fibrogenesis

Expression of RGD-binding integrin subunits was analyzed in mouse pancreas by real-time quantitative PCR after induction of pancreatic fibrogenesis by repeated cerulein treatment. Saline-treated mice served as controls. The expression of mRNA for all RGD-binding integrin subunits was detectable in the pancreas (Figure 1*A*). In control pancreas, we detected prominent expression of αv, α5, β1, and β5 subunit mRNAs, which is consistent with the possible expression of the following integrin heterodimers: avβ1, a5β1, and avβ5. Relatively lower expression of α8, β6, β3, and β8 mRNAs was detected, consistent with the possible expression of integrins α8β1, αvβ6, αvβ3, and αvβ8. Expression of all mRNA integrin subunits was induced

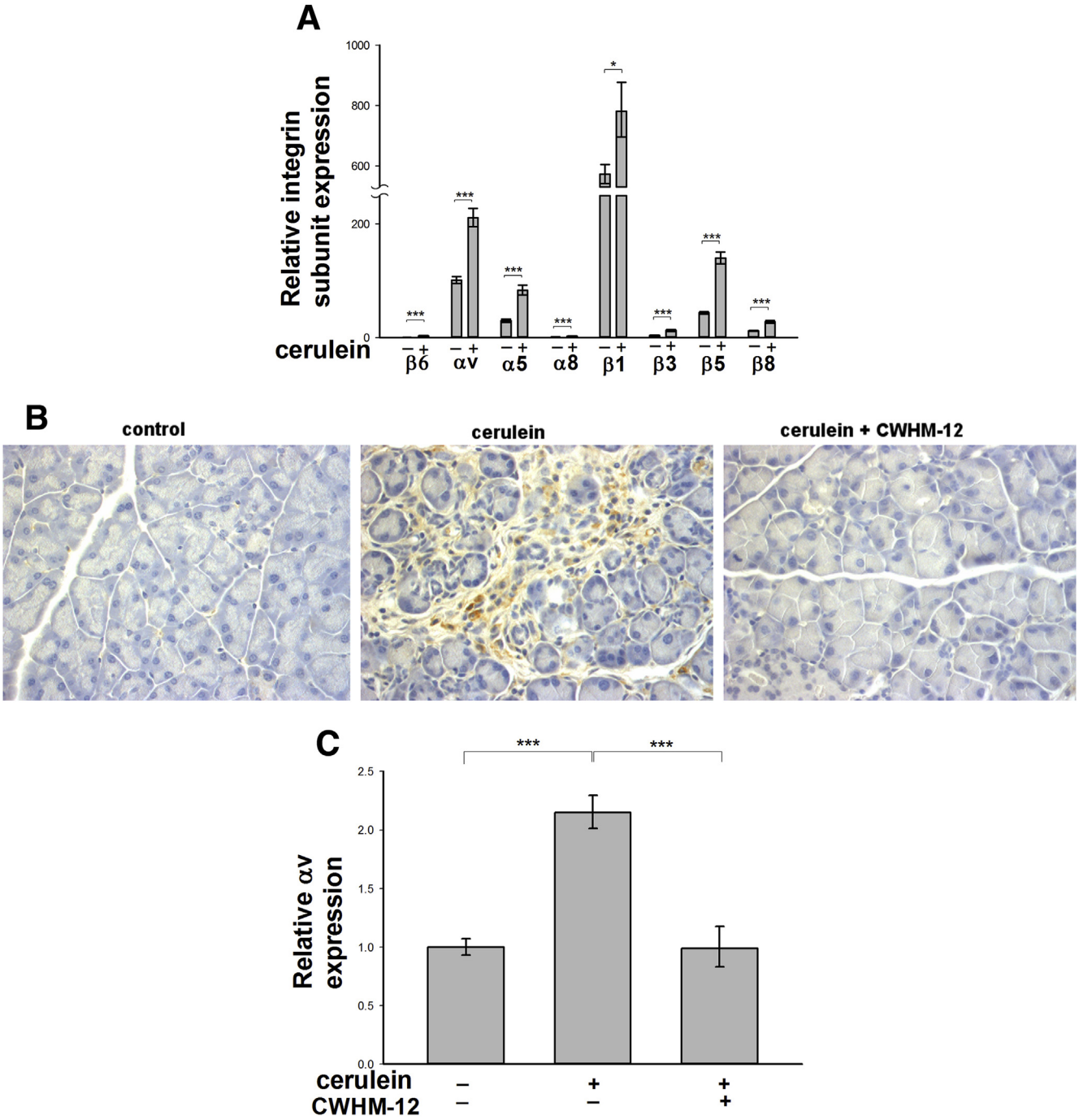

Figure 1. Expression of RGD-binding integrin subunits in mouse pancreas. Mice were subjected to repeated episodes of cerulein (+) or control saline (-) injections and killed on day 8 after the first injection. One group of mice was treated with CWHM-12 compound before cerulein and then throughout the studies as described in the Materials and Methods section. (*A*) Expression of RGD-binding subunits in control and cerulein-treated pancreas was measured by real-time quantitative PCR, normalized to the acidic ribosomal protein large P0, and depicted as the fold increase over the level of integrin β6 subunit expression in the control group of mice. Data are expressed as means ± SEM; n = 9. ***$P < .001$, *$P < .05$. (*B*) Representative immunostaining of pancreatic sections with an αv integrin subunit-specific antibody showed expression only in injured pancreas, and was reduced dramatically with CWHM-12 treatment. (*C*) Expression of integrin αV mRNA measured by real-time quantitative PCR and normalized to acidic ribosomal protein large P0 showed a reduction with CWHM-12 administration. Data are shown as the fold increase over the level in control group of mice (no cerulein treatment). Data are expressed as means ± SEM; n = 9. ***$P < .001$.

significantly with repetitive cerulein treatment. To investigate whether RGD-binding integrins play a role in the process of pancreatic fibrogenesis, we evaluated the broad-range RGD peptidomimetic integrin antagonist CWHM-12 in the cerulein injury mouse model of CP. CP was induced by repetitive administration of cerulein (days 1, 3, and 5), and pancreatic injury then was assessed on day 8 as described in the Materials and Methods section. CWHM-12 was delivered by continuous infusion at a dose of 100 mg/kg/day using minipumps implanted subcutaneously 3 days before the first cerulein treatment. At the end of the experiment, the steady-state plasma concentration of CWHM-12 in each mouse was determined by mass spectrometry analysis, and corresponded to 9.1 ± 3.2 μg/mL (mean ± SD). Because integrin subunit αv is a component of most of the RGD-binding integrins, the expression of this subunit was analyzed in mouse pancreases at the protein level by immunohistochemistry. Interestingly, we were able to detect αv integrin subunit only in injured cerulean-treated pancreases; preventive administration of integrin antagonist CWHM-12 produced no detectable αv expression (Figure 1*B*). Induction of pancreatic integrin αV mRNA expression induced by cerulein injury was similarly blocked by prophylactic administration of CWHM-12 compound (Figure 1*C*).

Preventive Administration of Integrin Antagonist CWHM-12 Attenuates Acinar Atrophy/Dropout in the Mouse Model of Pancreatic Fibrogenesis

The ratios of pancreatic weight to mouse body weight, as well as histologic changes, were evaluated to assess pancreatic atrophy, inflammation, and fibrosis. Pancreatic weights were significantly lower in the cerulein-treated groups than in control mice, indicating significant organ atrophy with repetitive injury. CWHM-12 treatment did not alter the effect of repetitive cerulein on pancreatic appearance or pancreatic weight (Figure 2*A* and *B*, respectively).

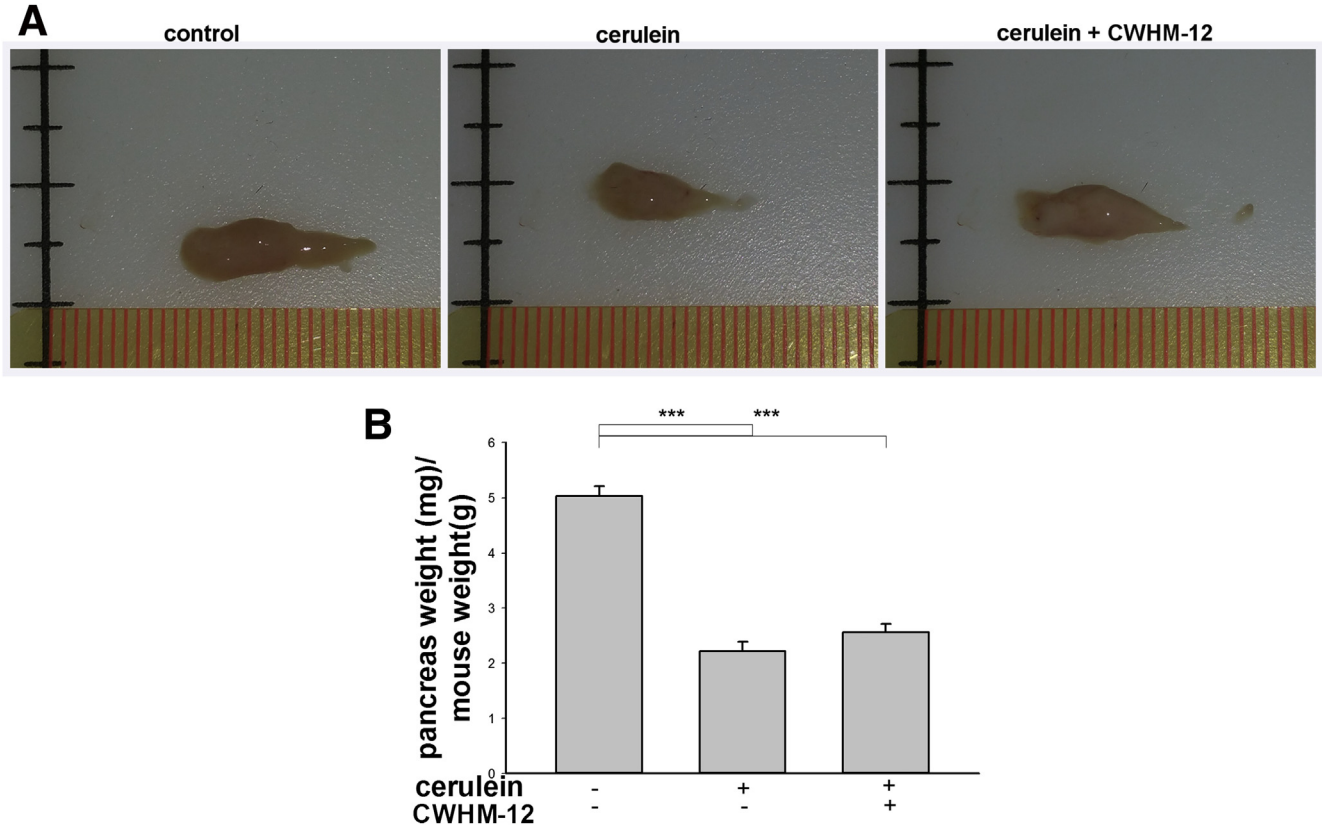

Figure 2. Effect of CWHM-12 administration on the severity of cerulein-induced repetitive pancreatic injury. (*A*) Macroscopic images of the pancreas before and after prophylactic administration of CWHM-12 compound. Representative picture shows that repetitive cerulein treatments affect the size of the pancreas, indicating substantial organ atrophy. CWHM-12 administration did not alter pancreatic atrophy significantly. (*B*) Pancreatic weight relative to total body weight in C57BL/6 mice after the induction of CP by repetitive cerulein treatment showed substantial atrophy at day 8. Data are expressed as means ± SEM; n = 9. *$P < .001$. (*C*) H&E staining of the pancreas from cerulein-treated mice shows disrupted acinar architecture, dedifferentiation to tubular complexes, and interstitial inflammation. CWHM-12 administration decreased acinar cell atrophy/dropout (see also Table 2). (*D*) Apoptotic cells in pancreas are increased significantly in cerulein-treated vs normal mice. (*E*) Apoptotic cells with acinar morphology are increased significantly in the cerulein-treated group. These cells were reduced with administration of CWHM-12, although this reduction did not reach statistical significance ($P = .1$). Data are presented as fold increase over the numbers of apoptotic acinar cells in saline treated mice and expressed as means ± SEM; n = 3. **$P < .01$.

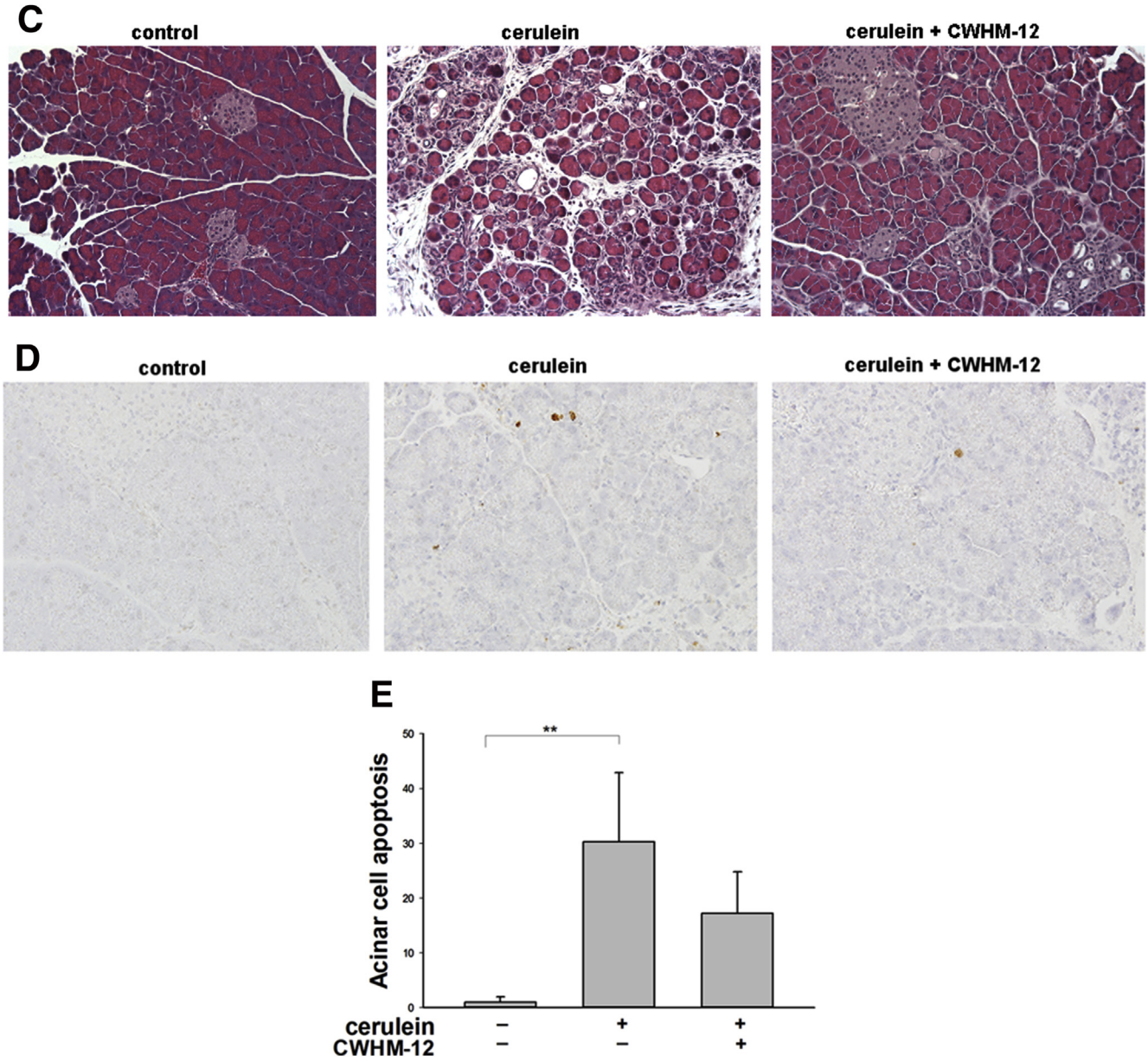

Figure 2. (*continued*).

Morphologic changes in the pancreas were assessed by H&E staining. Slides were analyzed by an experienced pathologist masked to treatment groups. Repetitive cerulein treatment caused significant morphologic alterations, including disruption of acinar cell architecture, infiltration with inflammatory cells, and development of tubular complexes. Preventive administration of CWHM-12 had no statistically significant effect on the formation of tubular complexes or infiltration of inflammatory cells. However, CWHM-12 application did decrease acinar cell atrophy/loss (Table 2), which was associated with a more normal overall appearance of the pancreatic tissue in H&E-stained sections (Figure 2*C*). To assess if the observed effect of CWHM-12 on acinar cell atrophy/loss was caused by decreased acinar cell apoptosis, we performed terminal deoxynucleotidyl transferase–mediated deoxyuridine triphosphate nick-end labeling staining of apoptotic cells in pancreatic tissues (Figure 2*D*). Apoptotic cells with acinar morphology were counted by an experienced pathologist masked to the treatment groups. Cerulein administration caused a significant increase in acinar apoptotic cells. CWHM-12 application reduced acinar apoptotic cells in pancreas, although this trend did not reach statistical significance (Figure 2*E*).

Preventive Administration of CWHM-12 Dramatically Reduced Pancreatic Collagen Deposition in the Cerulein Mouse Model of Pancreatic Fibrogenesis

Fibrosis in the pancreas was assessed by Sirius red staining as a measure of collagen deposition (Figure 3*A*). In control saline-treated mice, Sirius red staining was detected

Table 2. Effect of CWHM-12 Treatment on the Severity of Cerulein-Induced CP

Histopathology	No cerulein	Cerulein	Cerulein + CWHM-12
Necrosis	0 ± 0	0 ± 0	0 ± 0
Acinar atrophy/loss	0 ± 0	3.63 ± 0.32	2.33 ± 0.47[a]
Tubular complexes	0 ± 0	3.38 ± 0.38	2.56 ± 0.41
Acute inflammation	0 ± 0	1.63 ± 0.18	1.25 ± 0.24
Chronic inflammation	0 ± 0	2.38 ± 0.26	2.13 ± 0.12

NOTE. Histopathology was scored blindly as described in the Materials and Methods section. Higher values indicate greater severity. Data are expressed as means ± SEM. $n = 10$ mice per group.
[a]Acinar cerulein induction of CP was reduced significantly by CWHM-12 treatment ($P < .05$).

mostly around vessels and pancreatic ducts. Repetitive cerulein treatment strongly increased interlobular and periacinar staining, and this abnormal collagen deposition was decreased strikingly by CWHM-12 continuously administered before and during the injury-inducing regimen. These changes were quantified with morphometric image analysis (Figure 3*B*), which confirmed significant reduction of collagen staining with CWHM-12 treatment. Because expression of collagen type Iα1(I) (Col1a1) previously was reported to increase in pancreas of rodents with induced CP as well as in human beings with alcoholic pancreatitis,[37] we analyzed the expression of Col1a1 by real-time quantitative PCR. Pancreatic Col1a1 mRNA was induced significantly by cerulein, and this increase was prevented substantially by CWHM-12 treatment (Figure 3*C*). Because collagen levels in tissue could be affected by changes in degradation as well as synthesis, we evaluated the activity of MMP by gelatin zymography. MMP activity was increased significantly in pancreas with cerulein treatment, whereas CWHM-12-treated mice had slightly less activity (Figure 3*D*). Mmp2 mRNA showed a similar pattern of expression (Figure 3*E*).

Preventive Administration of CWHM-12 Attenuates PSC Activation in the Cerulein Mouse Model of Pancreatic Fibrogenesis

PSCs play a key role in extracellular matrix deposition and pancreatic fibrosis. In response to injury, PSCs develop an activated myofibroblast-like phenotype with increased α-SMA accumulation. To investigate if CWHM-12 affects activation of PSCs, we measured pancreatic α-SMA expression in our model. Pancreatic tissues from saline-treated control mice contained only normal perivascular positive cells and no interstitial α-SMA–positive staining cells, while pancreatic tissues from cerulein-treated mice contained α-SMA–positive cells in the periacinar spaces. CWHM-12 administration before and during the injury-inducing regimen dramatically decreased the appearance of α-SMA–positive staining (Figure 4*A*). To confirm and quantitate the results of α-SMA immunohistochemical staining, we conducted Western blot analysis of pancreatic extracts. This showed that α-SMA expression was increased significantly in cerulein-treated mice and that CWHM-12 treatment fully prevented it, resulting in α-SMA expression similar to control mice (Figure 4*B* and *C*). To gain insight into the mechanism of the CWHM-12–mediated decrease in α-SMA–positive PSCs, we analyzed the effect of CWHM-12 on total PSCs by measuring changes in the expression of vimentin, which is expressed in both activated and quiescent PSCs. The expression of vimentin in normal saline-treated mouse pancreases was undetectable, whereas pancreases from cerulein-treated mice were highly stained with vimentin antibody and coincided with anti–α-SMA antibody staining (Figure 4*D*). Pancreases from CWHM-12–treated mice had reduced but still significant levels of vimentin expression (Figure 4*E*); this suggests both decreased PSC activation and activated PSC dropout may account for the observed treatment-associated decrease in activated PSCs. The expression of vimentin mRNA also was assessed by real-time PCR, showing results similar to the protein pattern of expression (Figure 4*F*).

Preventive Administration of CWHM-12 Decreased Pancreatic TGFB Activation in the Cerulein Mouse Model of Pancreatic Fibrogenesis

p-SMAD3 measured by Western blot of pancreatic extracts was assessed as a measure of TGFB activation. This showed that p-SMAD3 was increased in pancreases from cerulein-treated mice, and that treatment with CWHM-12 prevented p-SMAD3 induction (Figure 5*A*).

We also assessed the expression of CTGF, because it is a downstream target of TGFB and is recognized as a mediator of the profibrogenic actions of TGFB, including pancreatic fibrogenesis in human beings and animals.[38] Real-time PCR showed CWHM-12 administration prevented the cerulein-induced up-regulation of this cytokine (Figure 5*B*). Because TGFB is known to inhibit leukocyte proliferation and activation, we performed hematologic analysis and found that white blood cells were increased slightly in the peripheral blood of compound-treated mice at study termination (Table 3). This further supports the concept that CWHM-12 treatment modulates TGFB function.

Therapeutic Administration of CWHM-12 Alleviates Collagen Deposition and PSC Activation in the Cerulein Mouse Model of Pancreatic Fibrogenesis

To assess if administration of CWHM-12 still could have an effect after fibrosis already is present (therapeutic mode), we implanted minipumps with CWHM-12 on day 5 of cerulein treatment, a time point when some fibrosis already has been established (Figure 6*A*), and then assessed subsequent changes in fibrosis in the pancreas on day 8. Compound CWHM-96, the inactive control enantiomer of CWHM-12, was used as a negative control. At the end of the experiment, the steady-state plasma concentrations of the

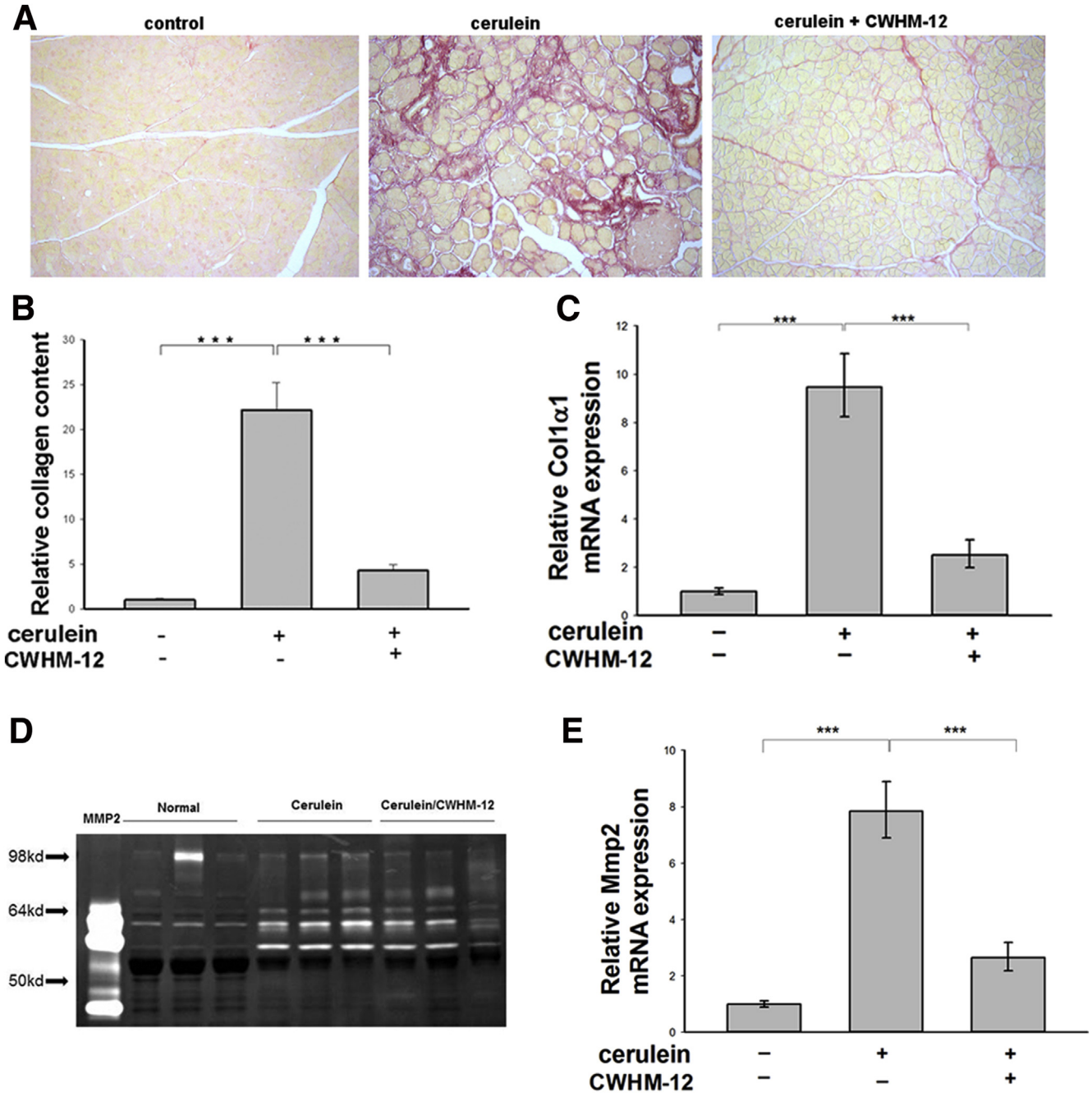

Figure 3. Effect of CWHM-12 on pancreatic collagen content in cerulein-treated mice. (*A*) Collagen accumulation in the pancreas assessed by Sirius red staining shows normal staining of perivascular and periductal stroma in the normal pancreas (*left*), extensive periacinar fibrosis in repetitive cerulein-treated animals (*center*), and substantial prevention of fibrosis in cerulein-treated animals that received CWHM-12 (*right*). (*B* and *C*) Data are shown as the fold increase over the level of the control group of mice (no cerulein treatment) and expressed as means ± SEM; n = 8. ***$P < .001$. (*B*) Quantification of Sirius red staining by morphometric analysis confirms the prevention of collagen accumulation by CWHM-12 administration. (*C*) Expression of Col1a1 mRNA measured by real-time quantitative PCR analysis and normalized to acidic ribosomal protein, large, P0 shows prevention of the increased procollagen mRNA by CWHM-12 treatment. (*D*) Effects of CWHM-12 administration on MMP enzyme activity in total pancreas. Gelatin zymography was performed with pancreas samples from normal mice that received intraperitoneal saline injections, mice that received the intraperitoneal cerulein injections, and mice that received cerulein injections while continuously treated with CWHM-12 delivered by osmotic minipumps. Purified recombinant mouse MMP-2 (2 ng) was included as a positive control for zymography. (*E*) Expression of MMP-2 mRNA measured by real-time quantitative PCR analysis and normalized to ribosomal protein, large, P0. Data are presented as the fold increase over the level of the control group of mice (no cerulein treatment) and expressed as means ± SEM; n = 8. ***$P < .001$.

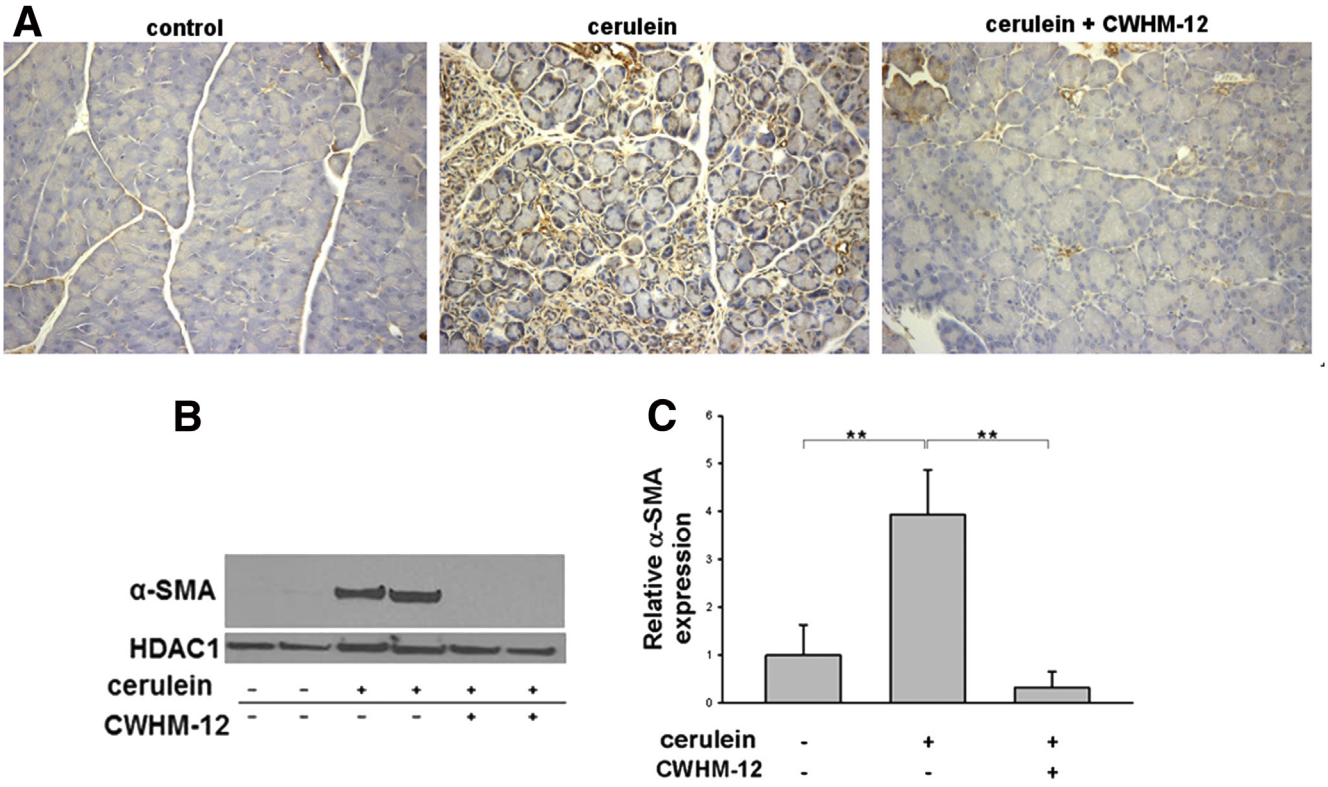

Figure 4. Effect of CWHM-12 on PSC activation in cerulein-treated mice. α-SMA was used as a marker of PSC activation. (*A*) Immunostaining of pancreatic sections with α-SMA–specific antibody shows normal perivascular staining in control pancreas (*left*), substantial periacinar staining after cerulein treatment (*center*), and prevention of PSC activation by CWHM-12 administration (*right*). (*B*) Representative Western blot of pancreatic extracts with α-SMA–specific antibody confirmed the differences seen histologically. Expression of α-SMA was normalized to the histone deacetylase 1 protein (HDAC1). (*C*) Densitometric analysis of α-SMA expression. Data are expressed as means ± SEM; n = 5. $^{**}P < .01$. (*D*) Vimentin was used as a marker of both quiescent and activated PSCs. Co-immunofluorescent staining of pancreatic sections with vimentin and α-SMA specific antibody was conducted as described in Materials and Methods. Representative picture demonstrates that normal control pancreases do not have expression of vimentin or α-SMA except for the α-SMA expression in smooth muscle cells surrounding blood vessel. After ceruein treatments, most of vimentin expressing PSC are α-SMA positive. (*E*) Immunostaining of pancreatic sections with vimentin-specific antibody showed high expression in pancreas of cerulein-treated mice, which was decreased partially with CWHM-12 administration. (*F*) Expression of vimentin mRNA measured by real-time quantitative PCR analysis and normalized to ribosomal protein, large, P0 shows a similar pattern of vimentin expression. Data are shown as the fold increase over the level of the control group of mice (no cerulein treatment) and expressed as means ± SEM; n = 9. $^{***}P < .001$, $^{**}P < .01$. DAPI, 4',6-diamidino-2-phenylindole; Vim, vimentin.

CWHM compounds in each mouse were determined by mass spectrometry. This confirmed effective delivery of both drugs with plasma concentrations of 6.1 ± 2.1 μg/mL (mean ± SD) for CWHM-12 and 13.7 ± 5.5 μg/mL for CWHM-96. Therapeutic CWHM-12 administration showed effective reduction of collagen accumulation induced by repetitive cerulein treatment by day 8 as assessed by Sirius red staining whereas treatment with CWHM-96 did not (Figure 6*A*). Results were quantified and confirmed by morphometric analysis (Figure 6*B*). Consistent with the histologic findings, administration of CWHM-12 also significantly reduced cerulein-induced pancreatic Col1a1 mRNA expression in the therapeutic mode. Treatment with the inactive control compound CWHM-96 had no significant effect (Figure 6*C*). To evaluate if the decrease in collagen accumulation was associated with decreased PSC activation, we analyzed the expression of the activated PSC marker α-SMA in the treatment groups by immunohistochemistry and by real-time reverse-transcription PCR (Figure 6*D* and 6*E*). CWHM-12 treatment resulted in the nearly complete disappearance of activated PSCs. Vimentin expression, a marker of total PSCs, still was detected easily in this group, but was reduced significantly compared with the control group.

CWHM-12 Administration Does Not Change the Parameters of Cerulein-Induced Acute Pancreatic Injury in Mice

To evaluate the possibility that CWHM-12 administration might influence the degree of acute pancreatic injury induced by cerulein treatment, we evaluated its effect on the following parameters of pancreatic injury in the acute phase (9 hours after beginning injections): edema (ratio of

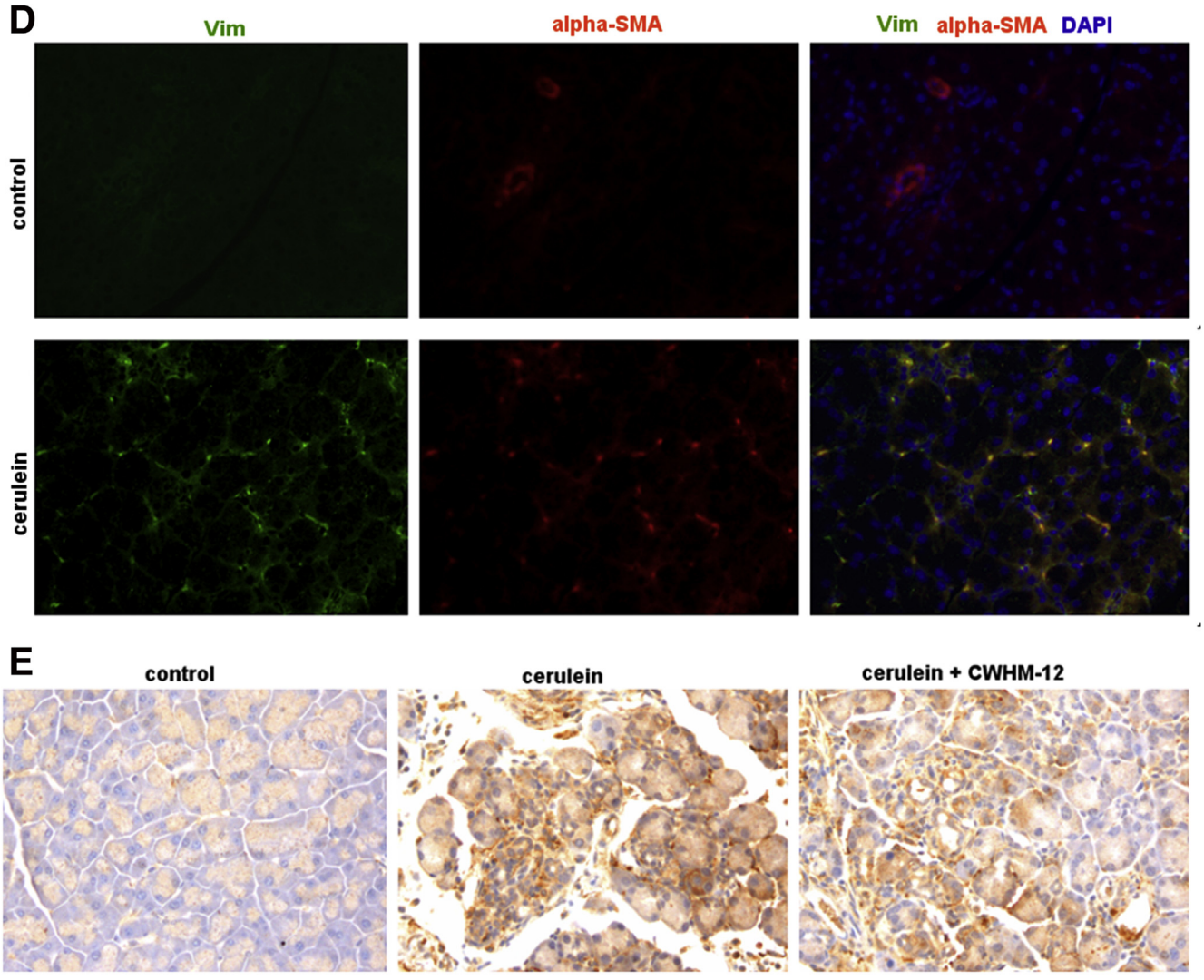

Figure 4. (*continued*).

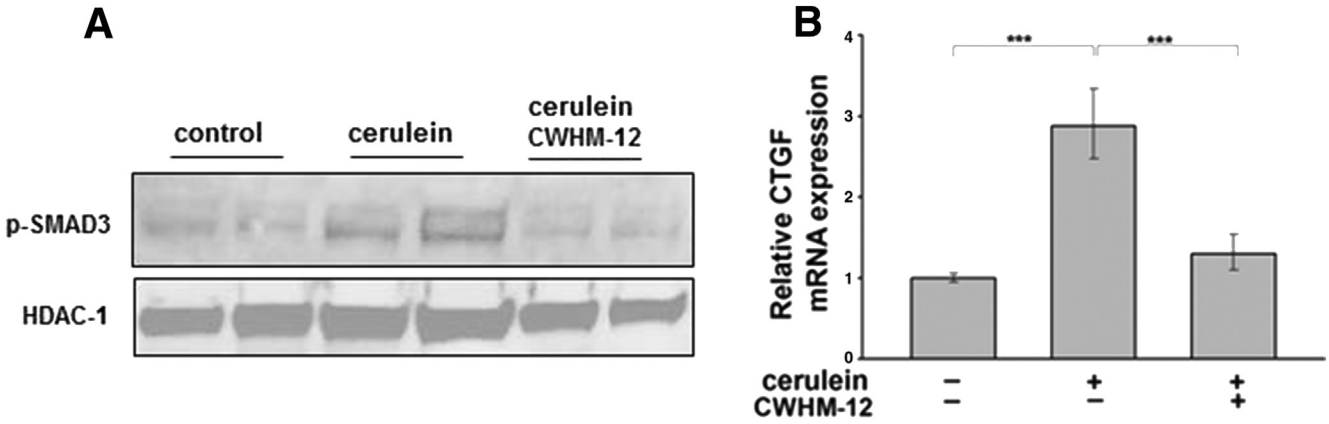

Figure 5. Effect of CWHM-12 on activated TGFB signaling in cerulein-treated mice. (*A*) Phosphorylation of SMAD3 was assessed as a measure of TGFB activation. Representative Western blot of pancreatic extracts with p-SMAD3–specific antibodies showed up-regulation with cerulein treatment, which was decreased to the level found in control pancreas after administration of CWHM-12. The histone deacetylase 1 protein (HDAC1) was used as a loading control. (*B*) CTGF expression was measured as a downstream target of TGFB signaling. CTGF mRNA expression was measured by real-time quantitative PCR, normalized to the ribosomal protein, large, P0 and shown as the fold increase over the level of CTGF expression in the control group of mice. CTGF expression was induced by repetitive cerulein administration and this increase was prevented by administration of CWHM-12. Data are expressed as means ± SEM; n = 9. ***$P < .001$.

pancreatic weight to mouse weight), plasma amylase activity, and histologic changes assessed on H&E-stained sections of the pancreas. Acute injury was induced as described in the Materials and Methods section. Pancreatic edema and plasma amylase levels increased considerably after acute pancreatic injury, but CWHM-12 treatment did not have significant effects on these parameters (Figure 7*A* and *B*). Histologic manifestations of acute pancreatitis (Figure 7*C*) were assessed by blinded scoring of 4 slides per treatment group at 9 hours after the first cerulein injection and also were not affected significantly by CWHM-12 administration (acinar necrosis, 2.0 ± 0 vs 2.0 ± 0; vacuolization, 1.5 ± 0.29 vs 1.25 ± 0.25; inflammatory cell infiltration, 2 ± 0 vs 1.0 ± 0.58; edema, 1 ± 0 vs 1 ± 0 in cerulein-treated and cerulein plus CWHM-12–treated mice, respectively). Similar to our findings in the chronic pancreatitis experiment, hematology analysis showed no significant changes in white blood cell count between control and cerulein-treated groups, although these were increased in the cerulein/CWHM-12 group (Table 3). These findings support the notion that inhibition of RGD-binding integrins is antifibrotic and not anti-inflammatory, consistent with contrasting roles of TGFB in these processes.

Subunits of RGD-Binding Integrins Are Expressed in Mouse Primary PSCs and Are Induced With PSC Activation

To identify which RGD-binding integrins are expressed specifically on PSCs and infer their potential roles in the process of pancreatic fibrogenesis, we first analyzed the expression of RGD-binding integrin subunits in quiescent primary mPSCs that were isolated as described in the Materials and Methods section. Quiescent PSCs comprise only a tiny portion (approximately 3%) of total pancreatic cells, therefore we pooled pancreases from 10 C57BL/6 mice for quiescent PSC isolation. By using quantitative real-time PCR, we showed that mRNA encoding all subunits of the RGD-binding integrins were present at varying levels in primary mPSCs. Expression was most prominent for the αv,

Table 3. Hematology Analysis of Terminal Blood Samples From Pancreatic Injury Studies

	Chronic model study			Acute model study		
Group	WBC	Lym	Neu	WBC	Lym	Neu
Control	7.1 ± 0.5	5.8 ± 0.4 (82)	1.2 ± 0.1 (16)	3.3 ± 0.3	1.8 ± 0.1 (1.8)	1.5 ± 0.2 (44)
Cerulein/veh	7.8 ± 0.5	6.4 ± 0.4 (81)	1.3 ± 0.1 (17)	2.5 ± 0.6	1.0 ± 0.3 (1.0)	1.5 ± 0.4 (60)
Cerulein/C 12	10.3 ± 0.7[a]	8.8 ± 0.7[a] (86)	1.3 ± 0.1 (13)	6.2 ± 0.8[a]	3.0 ± 0.8[a] (3.0)	3.1 ± 0.2[a] (55)

NOTE. Groups of mice were subjected to either saline (control) or cerulein intraperitoneal injections, and were given either vehicle (veh) or CWHM-12 (C12) delivered as described in the text for the chronic and acute models. Values are the mean ± SEM of cell counts ($\times 10^3/\mu L$) determined using a Cell-Dyn 3700 whole-blood analyzer. Numbers shown in parentheses are the percentage total white blood cells (WBCs) of lymphocytes (Lym) and neutrophils (Neu).
[a]$P < .05$ vs cerulein/veh.

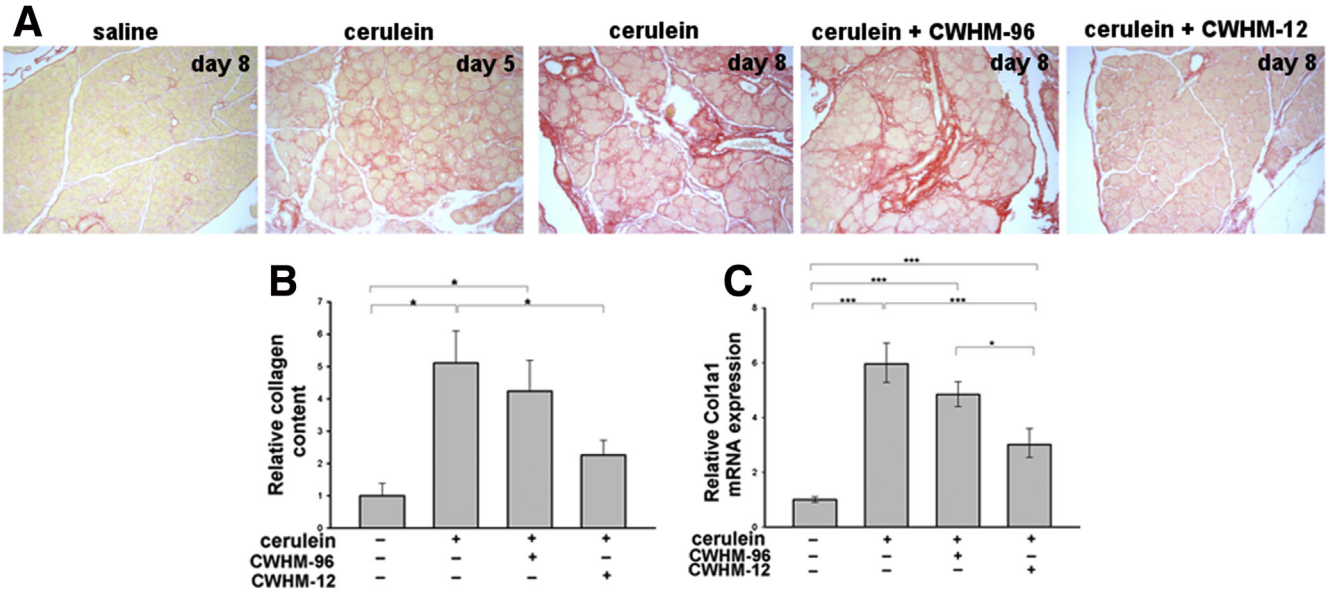

Figure 6. Analysis of collagen content in the cerulein model of pancreatic fibrogenesis after therapeutic administration of CWHM-12. (*A*) Collagen content of the pancreas assessed by Sirius red staining on various days after cerulein treatment. Saline-treated control mice showed no fibrosis. Representative Sirius red pancreatic staining from 5 mice killed on day 5 relative to the first cerulein treatment showed that some pancreatic fibrosis already was established. Eight days into the cerulein treatment regimen, further increase in fibrosis was apparent. Therapeutic treatment with the CWHM-96 control compound initiated on day 5 did not improve fibrosis whereas CWHM-12 treatment from day 5 significantly decreased fibrosis observed on day 8. (*B* and *C*) Data are shown as the fold increase over the level of the control group of mice (no cerulein treatment). Data are expressed as means ± SEM; n = 9. ***$P < .001$, *$P < .05$. (*B*) Quantification of Sirius red staining by morphometric analysis confirms the changes seen visually. (*C*) Expression of Col1a1 mRNA measured by real-time quantitative PCR analysis and normalized to acidic ribosomal protein, large, P0 showed a reduction in procollagen mRNA with CWHM-12 treatment. (*D*) α-SMA was used as a marker of PSC activation and was analyzed by immunohistochemistry. Representative picture of pancreatic sections with α-SMA–specific antibody shows blocking of cerulein-induced PSC activation by CWHM-12 treatment. (*E*) Expression of α-SMA and vimentin (Vim) mRNA measured by real-time quantitative PCR analysis and normalized to ribosomal protein, large, P0. Data are shown as the fold increase over the level of the control group of mice (no cerulein treatment) and are expressed as means ± SEM; n = 9. ***$P < .001$, *$P < .05$.

α5, β1, and β5 subunits, whereas expression of the β6 and α8 subunits was extremely low (Figure 8*A*). In an independent experiment, PSCs were isolated from 10 C57BL/6 mice and activated in culture as described in the Materials and Methods section. To assess whether expression of integrin subunits changes with the state of PSC activation, we deactivated PSCs in culture by serum starvation for 48 hours. This treatment is known to produce a state of relative quiescence in cultured hepatic and pancreatic stellate cells.[39] After serum starvation, culture media containing 10% FBS was re-introduced for 24 hours, a treatment that increases the activation of PSCs and their expression of α-SMA and profibrogenic genes. We found the integrin expression profile in just-isolated primary quiescent PSCs resembled the profile of primary mPSCs grown in culture and deactivated by serum withdrawal. Activation of mPSCs was associated with a significant increase in expression of integrin subunits αv, β1, and α5, whereas the quiescent state was associated with greater β5 and β8 expression (Figure 8*B*). We also found expression of α-SMA was increased significantly with serum treatment, confirming activated status of mPSCs under this condition (Figure 8*C*).

CWHM-12 Treatment Blocks TGFB Activity and Decreases Activation Markers of a PSC Line In Vitro

To investigate whether the antifibrotic mechanism of CWHM-12 involves inhibition of TGFB activation specifically by PSCs, we developed an in vitro system to study TGFB activation in PSCs. The use of primary mouse PSCs for in vitro studies is impractical because of extremely low yield and a very limited numbers of passages can be performed in culture. Therefore, we used an immortalized rat PSC line, LTC-14, for this purpose. These immortalized cells have all of the cardinal characteristics of activated PSCs such as vimentin expression showing the mesenchymal origin of the cells and a high level of α-SMA expression.[35] To determine if LTC-14 PSCs were capable of activating TGFB, we co-cultured these cells with a well-known MLEC reporter line that was designed for the sensitive detection of TGFB activity.[34] MLECs express a luciferase reporter gene under the control of the plasminogen activator inhibitor 1 TGFB-sensitive promoter. Co-culture of LTC-14 cells with the MLEC reporter cell line led to a substantial increase in luciferase activity (Figure 9*A*). Exogenous addition of a TGFB-neutralizing antibody, but not an isotype-matched

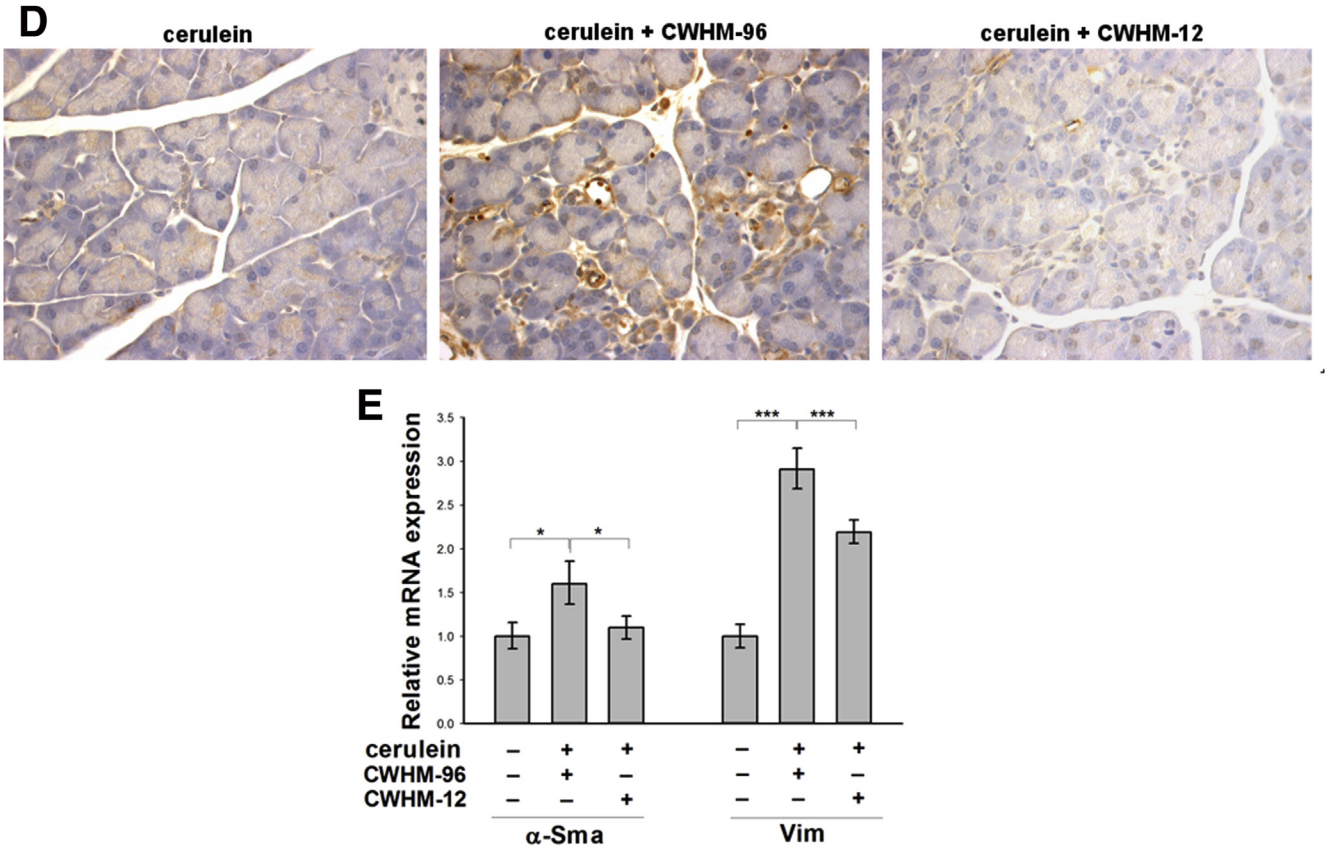

Figure 6. (*continued*).

negative control antibody, significantly diminished the luciferase activity, confirming the specificity of this assay for TGFB (Figure 9*A*). We then evaluated the effects of the integrin antagonist compound CWHM-12 on TGFB activation. We found that CWHM-12 potently blocked TGFB activation by the PSC cell line with a mean IC_{50} value of approximately 1.5 nmol/L (SD, 0.78; average, 4 independent experiments). A representative inhibition curve is shown in Figure 9*B*. In contrast, the negative control enantiomer CWHM-96 had no effect on inhibition of TGF-β activation by the PSCs in this assay, even at 1000-fold higher concentrations (data not shown). A separate study showed that protein expression of the downstream TGFB target α-SMA, also a marker of PSC activation, was reduced in cell culture by incubation with CWHM-12 for 48 hours (Figure 9*C* and *D*). MMP activity measured in cell lysates also was reduced (Figure 9*E* and *F*). These changes align with our observations from in vivo studies described earlier.

Discussion

Fibrosis is the major pathologic component of CP and provides the background milieu for the development of pancreatic cancer.[1,40] No disease-specific treatment is available. PSCs are the major source of extracellular matrix (ECM) that accumulates during pancreatic fibrogenesis.[4,41] It now is well established that TGFB and its downstream effector CTGF are the main cytokines responsible for stimulating the synthesis and secretion of ECM proteins by PSCs.[5] The pleotropic cytokine TGFB is regulated at many levels but probably the most important step in TGFB regulation is its extracellular activation.[7] The mechanism of TGFB activation in pancreatic fibrotic diseases is unknown. Recent data have indicated that in many organ injury states that lead to fibrosis, members of the RGD-binding integrin-receptor family appear to be the primary mediators of latent TGFB activation in vivo. [9–11] Besides activation of TGFB, RGD-binding integrins mediate other functions such as angiogenesis or ECM remodeling, as well as the migration of many cell types, which we speculate also are likely to be important at various stages of the initiation, development, maintenance, and resolution of fibrosis.[42,43]

In this study, we evaluated the role of RGD-binding integrins in the development of pancreatic fibrogenesis. By using quantitative real-time PCR analysis, we showed the expression of the subunits of RGD-binding integrins in the mouse pancreas and showed all were increased after the induction of CP. Expression of β6 and α8 subunits was very low even after CP induction. Because these subunits only form heterodimers with the αv and β1 subunits, respectively, these data suggest integrins $\alpha v\beta 6$ and $\alpha 8\beta 1$ are not prominent in either the normal or injured pancreas. These data would not preclude the possibility of their significant expression in small subpopulations of the total cells in pancreas. Expression of the αv integrin subunit was easily detectable at the mRNA and protein levels in fibrotic but

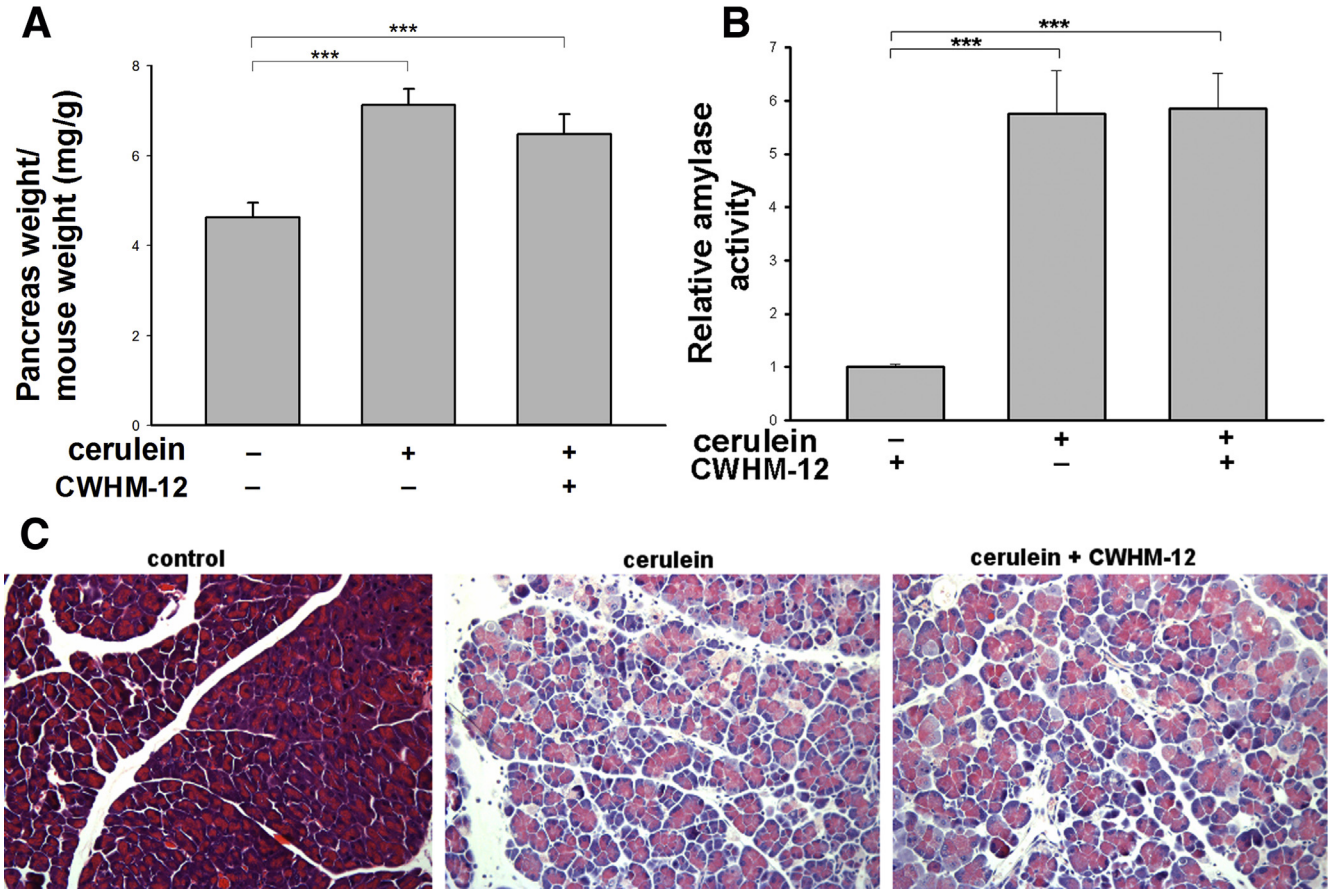

Figure 7. Effect of CWHM-12 administration on the severity of cerulein-induced acute pancreatic injury. (*A*) CWHM-12 administration did not affect pancreatic edema (measured as the ratio of pancreatic weight to body weight) in cerulein-treated mice. Data are expressed as means ± SEM; n = 5. ***$P < .001$. (*B*) CWHM-12 administration did not affect plasma amylase levels induced by cerulein treatment. Data are expressed as means ± SEM; n = 5. ***$P < .001$. (*C*) Representative (of 4 mice per group) H&E staining of mouse pancreatic sections. Pancreas from cerulein-treated mice showed acute injury including vacuolization, inflammatory cell infiltration, necrosis, and edema. CWHM-12 did not affect these parameters (see the Results section for quantitation).

not in normal pancreases, and protein was reduced to an undetectable level by treatment with CWHM-12. The αv subunit forms heterodimers with multiple β subunits to form several RGD-binding integrins, so the compound has the potential to affect functions of all of these expressed integrins simultaneously.

Our pharmacologic inhibitory approach based on the use of the potent synthetic nonpeptide broad-spectrum RGD peptidomimetic compound CWHM-12 allows direct functional evaluation of the importance of the whole group of RGD-binding integrins that are expressed in pancreas, both in normal mice and in mice with hyperstimulation-induced acute or chronic pancreatitis. As shown previously, CWHM-12 has high potency in blocking in vitro ligand binding to 4 of the TGFB-activating αv subunit-containing integrins (αvβ1, αvβ3, αvβ6, and αvβ8), and also has moderate potency against the TGFB-activating integrin αvβ5.[11] Our previous data also showed that CWHM-12 is a highly potent inhibitor of α5β1, an RGD-binding integrin, which has not been implicated in TGFB activation, but has known involvement in processes that are associated with fibrosis such as angiogenesis, cellular migration, and CTGF binding. We found that except for a slight prevention of cerulein-induced acinar cell atrophy/loss, CWHM-12 administration did not affect acinar cell morphology or inflammatory cell infiltration. However, it did dramatically suppress pancreatic fibrosis when administered prophylactically in the cerulein-induced CP model. We speculate that the modest improvement in acinar cell atrophy/loss could result from a decreased rate of acinar cell apoptosis because previous studies have shown that apoptosis plays an essential role in acinar cell loss in chronic pancreatitis,[44] and it also was shown that inhibition of TGFB1 action protects acinar cells from apoptosis in the cerulein model of chronic pancreatic injury.[22] Indeed, our analysis showed a significant increase in acinar cell apoptosis in the cerulein-treated group vs normal pancreas, and a trend toward reduction in apoptotic cells with CWHM-12 treatment. Pancreatic collagen content measured by Sirius red staining was decreased by more than 80% relative to vehicle-treated mice. This degree of fibrosis prevention in the CP model exceeds that seen in our similar recent studies in which preventive CWHM-12

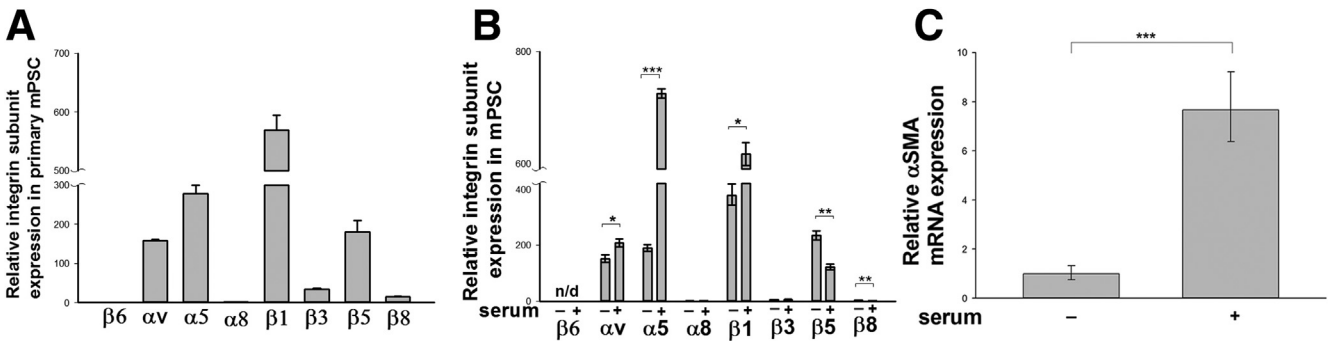

Figure 8. Expression of RGD-binding integrin subunits in mouse primary PSCs. (*A*) Primary mouse quiescent PSCs were isolated as described in the Materials and Methods section and subjected to real-time reverse-transcription PCR to detect the expression of mRNA encoding integrin subunits. Expression is shown as the fold increase over the level of β6 subunit. (*B* and *C*) Data are expressed as means ± SEM; n = 3. ***$P < .001$, **$P < .01$, *$P < .05$. (*B*) Primary mPSCs were expanded in culture as described in the Results section, and integrin subunit expression was compared between serum-deprived PSCs and serum-activated PSC growth conditions. Integrin subunit mRNA expression shown as the fold increase over the level of α8 subunits in the serum free–treated cells showed induction of the αv, α1, and β1 subunits with culture activation. (*C*) Decreased α-SMA mRNA expression in PSCs after serum deprivation supports de-activated status of PSC.

delivered at the same continuous dose in a mouse model of liver fibrosis produced less than a 50% decrease in collagen content.[11] CWHM-12–mediated reduction in pancreatic collagen content was accompanied by decreased PSC activation as assessed by expression analysis of α-SMA, the principal marker of PSC activation. CWHM-12 administration completely prevented an increase in α-SMA expression in the pancreas after cerulein injury, whereas in the previous mouse model of liver fibrosis, α-SMA expression was decreased by only approximately 35%.[11] Animals receiving the compounds by continuous infusion from minipumps consistently achieved steady-state plasma levels that far exceeded the concentrations that we showed fully inhibit integrin-mediated TGFB activation by PSCs and other cells in vitro. Therefore, we consider it unlikely that observed differences in efficacy between models are associated with variations in pharmacokinetic exposure. Instead, the more potent effect of CWHM-12 in preventing pancreatic compared with liver fibrosis supports the concept that the roles of RGD-binding integrins in fibrosis are to some extent tissue-, cell-, and/or injury-specific.[10]

Our observation that cerulein-injured pancreases in CWHM-12–treated mice contained almost no detectable α-SMA–positive PSCs could be owing to severe blockade of PSC activation, severe loss of activated PSCs, or a combination of these mechanisms. CWHM-12 treatment did not completely prevent the appearance of vimentin-positive cells. This suggests that PSCs proliferated in response to injury but were unable to complete their activation program owing to a lack of sufficient TGFB signaling. However, we hypothesize the drug also promotes loss of activated PSCs that do form because the level of vimentin-stained cells was clearly lower in cerulein-injured pancreases with CWHM-12 treatment.

Matrix metalloproteinase expression and activity were decreased by CWHM-12 treatment in cerulein-injured mice, suggesting that a reduction in collagen synthesis, not increased collagen degradation, is accountable for reduced fibrosis. This result may stem from the near-complete absence in the drug-treated samples of activated PSCs, a potentially rich source of such proteases.[45] Future studies will be needed to elucidate more precisely the mechanism of the observed effect.

Prophylactic studies are useful to provide initial proof-of-concept and to help determine the maximal impact of targeting a pathway from the earliest stages of development of the pathology. However, therapeutic administration studies provide a more appropriate context to assess the potential for clinical relevance with respect to arresting or reversing established fibrosis. We found that CWHM-12, but not CWHM-96 control treatment, significantly reduced fibrosis even after some fibrosis already had been established. The R-enantiomer of CWHM-12, CWHM-96, is an excellent negative control comparator because it differs in structure from CHWM-12 only in the orientation of its carboxyl (CO_2H) group and was at least 100-fold less active than CWHM-12 in all integrin assays.[11]

Our data showing that SMAD3 phosphorylation, together with transcription of TGFB-inducible genes Col1a1 and CTGF,[38,46] was decreased significantly by preventive CWHM-12 administration are consistent with TGFB activation as a probable primary mechanism through which RGD-binding integrins regulate pancreatic fibrogenesis. However, to rule out the possibility that the efficacy was secondary to a possible compound-mediated effect in decreasing the severity of the initial acute pancreatic injury that precedes and serves as a stimulus for fibrosis development, we evaluated the effect of CWHM-12 treatment in acute pancreatic injury. No significant differences in acute injury responses were found between CWHM-12 and vehicle-treated mice assessed by analyzing changes in pancreatic edema, levels of plasma amylase activity, and histologic evaluation after one cerulein treatment (consisting of 6 hourly injections). The data showing that RGD-binding integrins are not implicated in the initial injury suggest potential future clinical utility for antagonists will be in treatment of fibrosis associated with chronic pancreatitis.

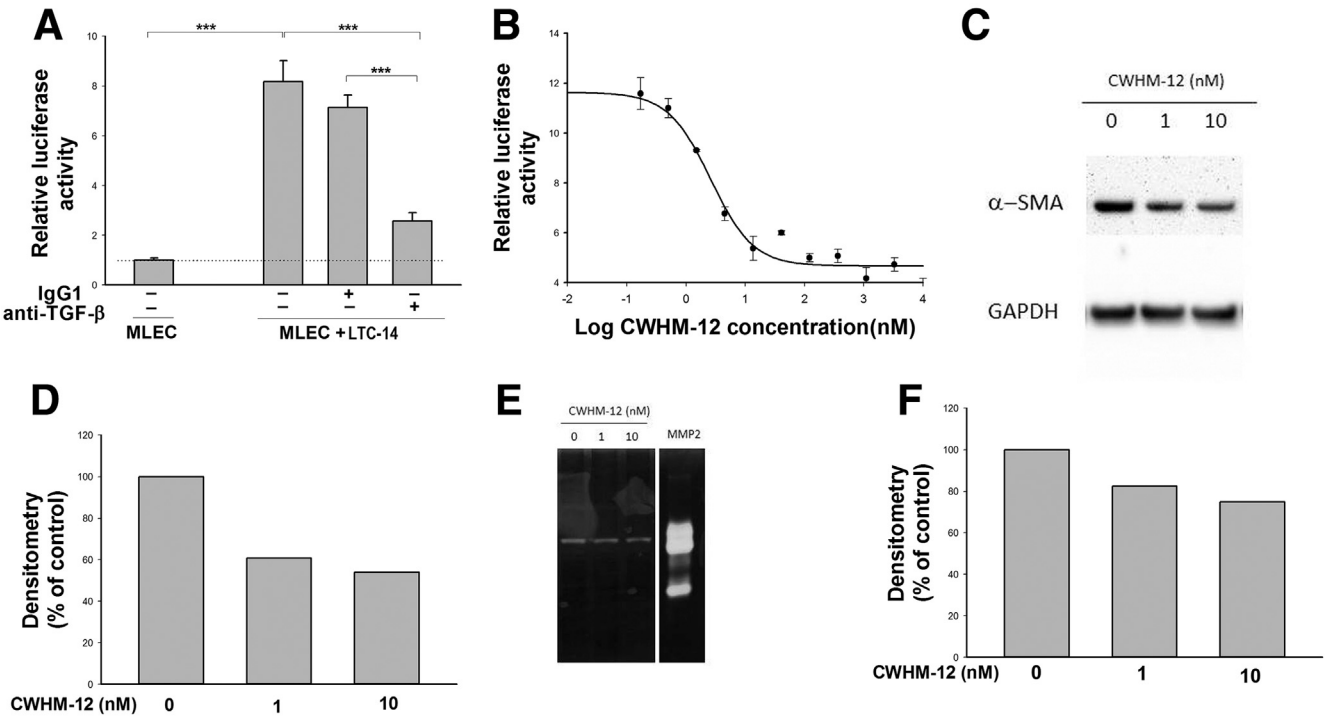

Figure 9. Effect of CWHM-12 administration on TGFB activity and activation markers of a PSC line in vitro. (*A*) Co-culture of TGFB reporter MLECs with LTC-14 PSCs increased luciferase reporter activity, indicating activation of latent TGFB. Neutralizing TGFB antibody, but not an isotype control IgG1 antibody, inhibited this activation, confirming that the observed increase in luciferase activity is TGFB dependent. Data are shown as the fold increase over the level of luciferase activity in MLECs alone and expressed as means ± SEM; n = 3. ***$P < .001$. (*B*) Concentration-dependent inhibition of integrin-mediated TGFB activation in LTC-14 by CWHM-12. The IC_{50} value calculated from the inhibition curve for CWHM-12 was 2.5 nmol/L. Luciferase activity on the graph is presented as the fold increase over the luciferase activity of MLECs cultured alone. Data are shown as means ± SEM; n = 3. (*C*). Representative picture of α-SMA protein expression in LTC-14 detected by Western blot showed a decrease in α-SMA expression with CWHM-12 treatment. (*D*) Densitometry analysis of α-SMA expression normalized to GAPDH. (*E*) Effect of CWHM-12 administration on gelatinase activity of LTC-14 PSCs. Gelatinase activity was detected by zymography. Purified recombinant MMP-2 (2 ng) was included as a positive control. (*F*) Densitometry analysis of MMP activity. GAPDH, glyceraldehyde-3-phosphate dehydrogenase.

A group of RGD-binding integrins expressed specifically on myofibroblasts was implicated previously in the development of fibrosis in the mouse liver, lung, and kidney.[11] As a first step in understanding the mechanism of integrin effects on TGFB activation in pancreatic cell types, we analyzed the expression of RGD-binging integrin subunits on primary PSCs, the major cell type responsible for ECM deposition in this organ. We detected the expression of all subunits of the RGD-binding integrins in primary quiescent mPSCs. The expression of integrin subunits β6 and α8 was extremely low. This finding is consistent with those of other investigators showing that fibroblasts are largely devoid of αvβ6 integrin.[47,48] Interestingly, the expression of α5, αv, and β1 subunits was induced with mPSC activation. The expression of α5β1 was reported previously in rat PSCs and was shown to be involved in CTGF signaling.[43] To evaluate whether RGD-binding integrins play a role in TGFB activation by PSCs, we developed a co-culture assay using a characterized PSC cell line and a widely used TGFB reporter cell line. We showed that the PSC line could robustly activate endogenously produced TGFB, and that CWHM-12, but not the control CWHM-96, compound potently blocked TGFB activation in this assay. This finding strongly supports a mechanism of TGFB activation by PSC-expressed RGD-binding integrins as a major mediator of pancreatic fibrogenesis.

References

1. Witt H, Apte MV, Keim V, et al. Chronic pancreatitis: challenges and advances in pathogenesis, genetics, diagnosis, and therapy. Gastroenterology 2007;132:1557–1573.
2. Apte MV, Haber PS, Applegate TL, et al. Periacinar stellate shaped cells in rat pancreas: identification, isolation, and culture. Gut 1998;43:128–133.
3. Bachem MG, Schneider E, Gross H, et al. Identification, culture, and characterization of pancreatic stellate cells in rats and humans. Gastroenterology 1998;115:421–432.
4. Omary MB, Lugea A, Lowe AW, et al. The pancreatic stellate cell: a star on the rise in pancreatic diseases. J Clin Invest 2007;117:50–59.
5. Apte MV, Pirola RC, Wilson JS. Pancreatic stellate cells: a starring role in normal and diseased pancreas. Front Physiol 2012;3:344.

6. Wynn TA. Common and unique mechanisms regulate fibrosis in various fibroproliferative diseases. J Clin Invest 2007;117:524–529.
7. Annes JP, Munger JS, Rifkin DB. Making sense of latent TGFbeta activation. J Cell Sci 2003;116:217–224.
8. van Laethem JL, Deviere J, Resibois A, et al. Localization of transforming growth factor beta 1 and its latent binding protein in human chronic pancreatitis. Gastroenterology 1995;108:1873–1881.
9. Worthington JJ, Klementowicz JE, Travis MA. TGFbeta: a sleeping giant awoken by integrins. Trends Biochem Sci 2011;36:47–54.
10. Nishimura SL. Integrin-mediated transforming growth factor-beta activation, a potential therapeutic target in fibrogenic disorders. Am J Pathol 2009;175:1362–1370.
11. Henderson NC, Arnold TD, Katamura Y, et al. Targeting of alpha v integrin identifies a core molecular pathway that regulates fibrosis in several organs. Nat Med 2013;19:1617–1624.
12. Hynes RO. Integrins: bidirectional, allosteric signaling machines. Cell 2002;110:673–687.
13. Asano Y, Ihn H, Yamane K, et al. Increased expression of integrin alpha(v)beta3 contributes to the establishment of autocrine TGF-beta signaling in scleroderma fibroblasts. J Immunol 2005;175:7708–7718.
14. Asano Y, Ihn H, Yamane K, et al. Involvement of alphavbeta5 integrin-mediated activation of latent transforming growth factor beta1 in autocrine transforming growth factor beta signaling in systemic sclerosis fibroblasts. Arthritis Rheum 2005;52:2897–2905.
15. Munger JS, Huang X, Kawakatsu H, et al. The integrin alpha v beta 6 binds and activates latent TGF beta 1: a mechanism for regulating pulmonary inflammation and fibrosis. Cell 1999;96:319–328.
16. Mu D, Cambier S, Fjellbirkeland L, et al. The integrin alpha(v)beta8 mediates epithelial homeostasis through MT1-MMP-dependent activation of TGF-beta1. J Cell Biol 2002;157:493–507.
17. Reed NI, Jo H, Chen C, et al. The alphavbeta1 integrin plays a critical in vivo role in tissue fibrosis. Sci Transl Med 2015;7:288ra79.
18. Hung CF, Mark N, Chow Y-H, et al. Role of integrin-a8 in bleomycin-induced lung injury. Ann Am Thorac Soc 2015;12:S74.
19. Neuschwander-Tetri BA, Bridle KR, Wells LD, et al. Repetitive acute pancreatic injury in the mouse induces procollagen alpha1(I) expression colocalized to pancreatic stellate cells. Lab Invest 2000;80:143–150.
20. Neuschwander-Tetri BA, Burton FR, Presti ME, et al. Repetitive self-limited acute pancreatitis induces pancreatic fibrogenesis in the mouse. Dig Dis Sci 2000;45:665–674.
21. Lerch MM, Gorelick FS. Models of acute and chronic pancreatitis. Gastroenterology 2013;144:1180–1193.
22. Nagashio Y, Ueno H, Imamura M, et al. Inhibition of transforming growth factor beta decreases pancreatic fibrosis and protects the pancreas against chronic injury in mice. Lab Invest 2004;84:1610–1618.
23. He J, Sun X, Qian KQ, et al. Protection of cerulein-induced pancreatic fibrosis by pancreas-specific expression of Smad7. Biochim Biophys Acta 2009;1792:56–60.
24. Yoo BM, Yeo M, Oh TY, et al. Amelioration of pancreatic fibrosis in mice with defective TGF-beta signaling. Pancreas 2005;30:e71–e79.
25. Ulmasov B, Xu Z, Tetri LH, et al. Protective role of angiotensin II type 2 receptor signaling in a mouse model of pancreatic fibrosis. Am J Physiol Gastrointest Liver Physiol 2009;296:G284–G294.
26. Ulmasov B, Xu Z, Talkad V, et al. Angiotensin II signaling through the AT1a and AT1b receptors does not have a role in the development of cerulein-induced chronic pancreatitis in the mouse. Am J Physiol Gastrointest Liver Physiol 2010;299:G70–G80.
27. Ulmasov B, Oshima K, Rodriguez MG, et al. Differences in the degree of cerulein-induced chronic pancreatitis in C57BL/6 mouse substrains lead to new insights in identification of potential risk factors in the development of chronic pancreatitis. Am J Pathol 2013;183:692–708.
28. Wang X, Seed B. A PCR primer bank for quantitative gene expression analysis. Nucleic Acids Res 2003;31:e154.
29. Lugea A, Gukovsky I, Gukovskaya AS, et al. Nonoxidative ethanol metabolites alter extracellular matrix protein content in rat pancreas. Gastroenterology 2003;125:1845–1859.
30. Gukovsky I, Gukovskaya AS, Blinman TA, et al. Early NF-kappaB activation is associated with hormone-induced pancreatitis. Am J Physiol 1998;275:G1402–G1414.
31. Perides G, Tao X, West N, et al. A mouse model of ethanol dependent pancreatic fibrosis. Gut 2005;54:1461–1467.
32. Livak KJ, Schmittgen TD. Analysis of relative gene expression data using real-time quantitative PCR and the 2(-delta C(T)) method. Methods 2001;25:402–408.
33. French SW, Miyamoto K, Wong K, et al. Role of the Ito cell in liver parenchymal fibrosis in rats fed alcohol and a high fat-low protein diet. Am J Pathol 1988;132:73–85.
34. Abe M, Harpel JG, Metz CN, et al. An assay for transforming growth factor-beta using cells transfected with a plasminogen activator inhibitor-1 promoter-luciferase construct. Anal Biochem 1994;216:276–284.
35. Sparmann G, Hohenadl C, Tornoe J, et al. Generation and characterization of immortalized rat pancreatic stellate cells. Am J Physiol Gastrointest Liver Physiol 2004;287:G211–G219.
36. Yuan JS, Reed A, Chen F, et al. Statistical analysis of real-time PCR data. BMC Bioinformatics 2006;7:85.
37. Haber PS, Keogh GW, Apte MV, et al. Activation of pancreatic stellate cells in human and experimental pancreatic fibrosis. Am J Pathol 1999;155:1087–1095.
38. Grotendorst GR. Connective tissue growth factor: a mediator of TGF-beta action on fibroblasts. Cytokine Growth Factor Rev 1997;8:171–179.

39. Neuschwander-Tetri BA, Talkad V, Stephen FO. Induced thrombospondin expression in the mouse pancreas during pancreatic injury. Int J Biochem Cell Biol 2006; 38:102–109.
40. Neesse A, Michl P, Frese KK, et al. Stromal biology and therapy in pancreatic cancer. Gut 2011;60:861–868.
41. Apte MV, Wilson JS, Lugea A, et al. A starring role for stellate cells in the pancreatic cancer microenvironment. Gastroenterology 2013;144:1210–1219.
42. Babic AM, Chen CC, Lau LF. Fisp12/mouse connective tissue growth factor mediates endothelial cell adhesion and migration through integrin alphavbeta3, promotes endothelial cell survival, and induces angiogenesis in vivo. Mol Cell Biol 1999;19:2958–2966.
43. Gao R, Brigstock DR. Connective tissue growth factor (CCN2) in rat pancreatic stellate cell function: integrin alpha5beta1 as a novel CCN2 receptor. Gastroenterology 2005;129:1019–1030.
44. Bateman AC, Turner SM, Thomas KS, et al. Apoptosis and proliferation of acinar and islet cells in chronic pancreatitis: evidence for differential cell loss mediating preservation of islet function. Gut 2002;50: 542–548.
45. Phillips PA, McCarroll JA, Park S, et al. Rat pancreatic stellate cells secrete matrix metalloproteinases: implications for extracellular matrix turnover. Gut 2003; 52:275–282.
46. Lindahl GE, Chambers RC, Papakrivopoulou J, et al. Activation of fibroblast procollagen alpha 1(I) transcription by mechanical strain is transforming growth factor-beta-dependent and involves increased binding of CCAAT-binding factor (CBF/NF-Y) at the proximal promoter. J Biol Chem 2002;277:6153–6161.
47. Breuss JM, Gillett N, Lu L, et al. Restricted distribution of integrin beta 6 mRNA in primate epithelial tissues. J Histochem Cytochem 1993;41:1521–1527.
48. Wang B, Dolinski BM, Kikuchi N, et al. Role of alphav-beta6 integrin in acute biliary fibrosis. Hepatology 2007; 46:1404–1412.

Received February 24, 2016. Accepted March 4, 2016.

Correspondence
Address correspondence to: Barbara Ulmasov, PhD, Edward A. Doisy Research Center, Saint Louis University, 1100 South Grand Boulevard, Saint Louis, Missouri 63104. e-mail: bulmasov@slu.edu; fax: (314) 977-9909.

Conflicts of interest
These authors disclose the following: Peter Ruminski and David Griggs are consultants and equity holders of Antegrin Therapeutics, Inc; and Brent A. Neuschwander-Tetri has been a consultant for Nimbus Therapeutics, Bristol Myers Squibb, Janssen, Mitsubishi Tanabe, Conatus, and Scholar Rock. The remaining authors disclose no conflicts.

Funding
Supported by a National Pancreas Foundation grant (B.U. and D.W.G.) and the Frank R. Burton Memorial Fund (B.U.).